

Cover Page



Universiteit Leiden



The handle <http://hdl.handle.net/1887/35771> holds various files of this Leiden University dissertation.

Author: Palm, Walter Miguel

Title: Ventricular dilatation in aging and dementia

Issue Date: 2015-09-29

VENTRICULAR DILATATION
IN AGING AND DEMENTIA

ISBN 978 94 6159 459 4
LAYOUT Datawyse / Universitaire Pers Maastricht
COVER illustration Shutterstock
PRINTED BY Datawyse / Universitaire Pers Maastricht

© W.M. PALM

Copyright of the individual chapters lies with the publisher of the journal listed at the beginning of each respective chapter. No part of this thesis may be reproduced in any form, by print, photocopy, digital file, internet, or any other means without written permission from the author.

VENTRICULAR DILATATION IN AGING AND DEMENTIA

PROEFSCHRIFT

ter verkrijging van
de graad van Doctor aan de Universiteit Leiden,
op gezag van Rector Magnificus prof.mr. C.J.J.M. Stolker,
volgens besluit van het College voor Promoties
te verdedigen op dinsdag 29 september 2015
klokke 11.15 uur

door

MIGUEL PALM

geboren te Valladolid
in 1978

PROMOTIECOMMISSIE

PROMOTOR

Prof. dr. M.A. van Buchem

COPROMOTORES

Dr. J. van der Grond

Dr. L.J. Launer, National Institute on Aging

OVERIGE LEDEN

Dr. M. Vernooij, Erasmus Medisch Centrum Rotterdam

Prof. dr. G.J. Blauw

Prof. dr. H.A.M. Middelkoop

Prof. dr. R.J. van Oostenbrugge, Maastricht Universitair Medisch Centrum

Prof. dr. V. Gudnason, University of Iceland

Table of Contents

Chapter 1	General Outline and Introduction	7
Chapter 2	MMSE scores correlate with local ventricular enlargement in the spectrum from cognitively normal to Alzheimer's disease. <i>NeuroImage. 2008;39(4):1832-8.</i>	15
Chapter 3	Cerebral atrophy in elderly with subjective memory complaints. <i>Journal of Magnetic Resonance Imaging.2013;38(2):358-64.</i>	29
Chapter 4	Intracranial compartment volumes in normal pressure hydrocephalus: volumetric assessment versus outcome. <i>American Journal of Neuroradiology. 2006;27(1):76-9.</i>	45
Chapter 5	Ventricular dilatation: association with gait and cognition. <i>Annals of Neurology. 2009;66(4):485-93.</i>	57
Chapter 6	Disproportionate ventricular dilatation in the elderly could be a manifestation of small vessel disease. <i>Submitted.</i>	75
	Summary and conclusions	87
	Samenvatting en conclusies	93
	Curriculum vitae	99
	Publication list	103

1

General Outline and Introduction

Introduction

The cerebral ventricular system consists of four interconnected ventricles containing cerebrospinal fluid (CSF). CSF is produced by a network of ependymal cells in the choroid plexus, which is located within the ventricles, and flows from the lateral ventricles through the foramina of Monro into the third ventricle, and subsequently through the cerebral aqueduct to the fourth ventricle (Figure 1.1). From there it either passes into the central canal of the spinal cord or into the cisterns of the subarachnoid space, via the central foramen of Magendie and the two lateral foramina of Luschka. The CSF is reabsorbed into the dural sinuses via arachnoid villi and enters the venous system. CSF provides buoyancy to the brain as well as protection from abrupt movements, facilitates the removal of waste metabolites, and has a role in the repair of the central nervous system.¹

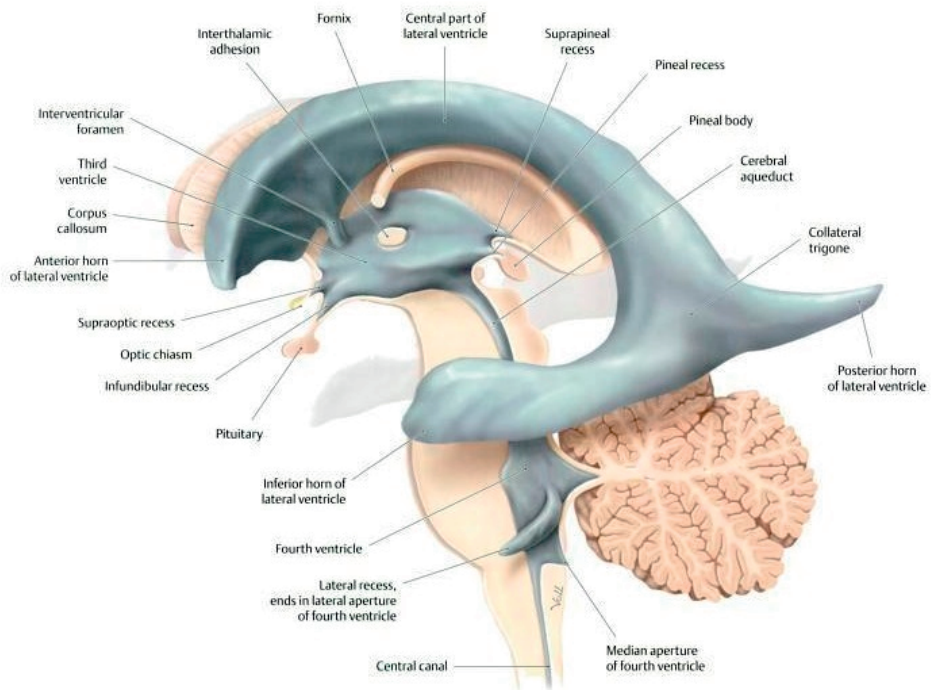


Figure 1.1 The cerebral ventricular system

Michael Schünke, Erik Schulte and Udo Schumacher, Thieme Atlas of Anatomy: Head and Neuroanatomy, Lawrence Ross, Edward Lamperti, Ethan Taub, 2006, copyrighted by Georg Thieme Verlag, Stuttgart, Germany, www.thieme.com (reprinted with permission)

CSF harbors information not yet tapped into. The distinction on Magnetic Resonance Imaging (MRI) between the cortical gray and subcortical white matter is known to decrease with aging. With a decrease in contrast between gray and white matter structures, volumetric assessment of brain structures that are not surrounded by CSF becomes more challenging. The sharp distinction between ventricles and brain parenchyma however is not influenced by aging, ensuring reliability of segmentation techniques despite older age. Ventricular shape and size may be analyzed as an indirect measure of cerebral atrophy.

Variations in ventricular shape and size are well known to exist in the normal population. Ventricular dilatation is one of the imaging hallmarks of the aging process. Abnormal ventricular enlargement may be divided into non-communicating (obstructive) and communicating hydrocephalus. Causes of non-communicating hydrocephalus may be congenital (aqueduct atresia / stenosis or posterior fossa malformations) or acquired (infectious, neoplastic or secondary to intracranial hemorrhage). Communicating hydrocephalus may be ex vacuo in response to brain parenchyma loss, for instance in cerebral atrophy or traumatic brain injury, or may be part of the syndrome of Normal Pressure Hydrocephalus (NPH, a triad of gait disorder, cognitive dysfunction and bladder dysfunction in the setting of disproportionate ventricular dilatation).

It is essential to differentiate between the expected ventricular dilatation in aging and abnormal ventricular changes. This differentiation can be challenging. Several methods have been devised to facilitate the distinction of normal and abnormal ventricular dilatation. Ventricular size can be measured using the frontal horn ratio (width of frontal horns divided by the internal diameter of the vault at the same level), bicaudate ratio (width of ventricles between caudate nuclei divided by the internal diameter of the vault at the same level) or Evans' index (width of frontal horns divided by the greatest internal diameter of the vault) on axial CT and MRI images.² More precise post-processing methods can segment brain tissue and CSF, after which a ventricle to brain ratio or ventricular to intracranial volume ratio can be calculated.

Differentiation between normal and abnormal ventricular enlargement is all the more relevant in the case of NPH, since a select number of patients with NPH may benefit from ventricular shunt surgery, making this one of the few potentially reversible dementia syndromes. In typical NPH there is a discrepancy between the volume of the ventricles and peripheral CSF volume, with disproportionate enlargement of the ventricular volume. No specific quantitative measure for disproportionate ventricular dilatation has yet been described.³ The prevalence of this particular type of ventricular

dilatation in the general population is not known, and the possible functional consequences are not clear.

The etiology of ventricular dilatation in NPH is not known. Early theories on altered CSF resorption have given way to thoughts on a vascular origin. The presence of reduced cerebral blood flow (CBF) in NPH is well established.^{4,5} Furthermore, intracranial vascular compliance was found to be significantly different in patients with NPH.⁶ The theoretical background to decreased intracranial vascular compliance leading to NPH was set out in a landmark paper from 2004, suggesting that decreased intracranial compliance causes restricted arterial pulsations and increased capillary pulsations, resulting in increased pulse pressure in the brain capillaries that maintain the ventricular enlargement in chronic communicating hydrocephalus.⁷ A later study proposed a “two hit” pathophysiology: “benign external hydrocephalus” in infancy followed by deep white matter ischemia in late adulthood.⁸ The problem with the placement of ischemia at the center of the etiology of NPH is that not all patients have ischemia.⁹ This was emphasized in a study based on PET/MRI data that found mean CBF to be reduced in NPH patients, but a standard deviation that was wide enough to theoretically place 16% of patients with NPH within the normal range.¹⁰ At present, altered hemodynamics seem to be the most plausible cause of NPH.⁹

NPH is not the only dementia syndrome with enlarged ventricles as an imaging feature, highlighting the need for additional tools to differentiate this condition from other diseases with a similar clinical presentation. Moreover, the most common dementia syndromes all have an element of atrophy in general, or ventricular dilatation in particular. Alzheimer’s disease (AD) is characterized by medial temporal lobe atrophy. In an advanced stage this results in dilatation of the temporal horn of the lateral ventricles.¹¹ Vascular dementia may lead to enlarged ventricles as a result of periventricular parenchymal loss due to ischemia or hemorrhage. Global cerebral atrophy in Parkinson’s disease and Dementia with Lewy Bodies, as well as frontotemporal atrophy in Frontotemporal dementia may all appear as ventricular dilatation.

Aims of this thesis

The general aim of this thesis was to study the causes and consequences of ventricular dilatation in aging and dementia. Additional objectives to support this aim were to design a measure that may objectively quantify the disproportionate ventricular dilatation that is characteristic to NPH, to study the value of such a measure for the

selection of candidates with NPH for ventricular shunting, to study the shape and size of the ventricles in relation to dementia syndromes, and to investigate potential new MRI markers of cognitive decline in both aging and AD.

Outline of this thesis

In an exploratory study prior to this thesis we searched for potential ventricular shape based biomarkers to discriminate between patients with AD and healthy elderly. An innovative technique for fully automatic shape modeling was applied to generate comparable meshes of all ventricles, permitting a point-by-point comparison of the ventricular surface. Potential biomarkers were then used to build an intelligent machine for AD detection, which was subsequently tested on previously unseen cases.

Building on evidence of focal atrophy of periventricular structures in AD in said study, the same method of modeling and analyzing local shape variations of ventricles was applied to a wider spectrum of cognitive levels in chapter 2. Each participant was assessed with the Mini-Mental State Examination, yielding a study sample ranging from cognitively healthy to mild cognitive impairment, and from mild to advanced AD. The severity of periventricular atrophy was estimated as local enlargement of the ventricular surface relative to an average normal subject, and the extent of atrophy was defined as the percentage of the ventricular surface significantly different from an average control. Linear regression across subjects was performed to evaluate the correlation between atrophy and MMSE score.

In chapter 3 the method of ventricular shape modeling was directed towards investigating possible local shape differences between cognitively healthy and persons with subjective memory complaints. Subjective memory complaints are common in the elderly, and are considered to be part of the spectrum that ranges from normal cognition to dementia. Though the memory complaints cannot be substantiated with formal cognitive testing, previous publications described cerebral atrophy on MR images of elderly with memory complaints, as well as AD type pathology on postmortem examinations.¹²

Shunt surgery remains the standard treatment for NPH, despite high morbidity rates and lack of evidence indicating that shunt placement is effective in the management of this condition. Many diagnostic procedures have been described that may increase the probability of selecting the appropriate candidates for shunt surgery. In chapter 4 we studied the potential of volumetric assessment to distinguish between patients who

respond to ventricular shunt surgery and those who do not. The preoperative ratio of ventricular volume and sulcal CSF volume was correlated with postoperative improvement in gait impairment, cognitive impairment, and bladder function.

In chapter 5 we investigated the prevalence of disproportionate ventricular dilatation (expressed as the upper quartile of the ratio of ventricular volume and sulcal CSF volume) in a cohort of elderly persons from the general population. In addition, we studied the association of disproportionate ventricular dilatation with symptoms from the NPH triad, consisting of gait impairment, cognitive impairment, and urinary incontinence. Since patients with white matter hyperintensities (WMH) or subcortical arteriosclerotic encephalopathy often present with an enlarged ventricular system and symptoms similar to those seen in NPH, the associations were adjusted for WMH volume and cardiovascular risk factors.

Elaborating on earlier studies that suggested a vascular origin of disproportionate ventricular dilatation in NPH, in chapter 6 we hypothesized that ventricular volume out of proportion to sulcal CSF volume is caused by white matter atrophy resulting from small vessel disease. In order to quantify disproportionate ventricular dilatation, we used the ratio of ventricular volume and sulcal CSF volume. Small vessel disease was expressed as WMH volume. Linear regressions were used to study the relationship between WMH volume, ventricular volume, sulcal CSF volume, and the ratio of ventricular volume and sulcal CSF volume.

References

1. Redzic ZB, Preston JE, Duncan JA, Chodobski A, Szmydynger-Chodobska J. The choroid plexus-cerebrospinal fluid system: from development to aging. *Current Topics in Developmental Biology* 2005;71:1-52.
2. Kiroglu Y, Karabulut N, Oncel C, Yagci B, Sabir N, Ozdemir B. Cerebral lateral ventricular asymmetry on CT: how much asymmetry is representing pathology? *Surgical and Radiologic Anatomy* 2008;30:249-55.
3. Toma AK, Holl E, Kitchen ND, Watkins LD. Evans' index revisited: the need for an alternative in normal pressure hydrocephalus. *Neurosurgery* 2011;68:939-44.
4. Kristensen B, Malm J, Fagerland M, et al. Regional cerebral blood flow, white matter abnormalities, and cerebrospinal fluid hydrodynamics in patients with idiopathic adult hydrocephalus syndrome. *Journal of Neurology, Neurosurgery, and Psychiatry* 1996;60:282-8.
5. Owler BK, Pickard JD. Normal pressure hydrocephalus and cerebral blood flow: a review. *Acta Neurologica Scandinavica* 2001;104:325-42.
6. Bateman GA. Vascular compliance in normal pressure hydrocephalus. *AJNR American Journal of Neuroradiology* 2000;21:1574-85.
7. Greitz D. Radiological assessment of hydrocephalus: new theories and implications for therapy. *Neurosurgical Review* 2004;27:145-65; discussion 66-7.
8. Bradley WG, Jr., Bahl G, Alksne JF. Idiopathic normal pressure hydrocephalus may be a "two hit" disease: benign external hydrocephalus in infancy followed by deep white matter ischemia in late adulthood. *Journal of magnetic resonance imaging : Journal of Magnetic Resonance Imaging* 2006;24:747-55.
9. Bateman GA. The pathophysiology of idiopathic normal pressure hydrocephalus: cerebral ischemia or altered venous hemodynamics? *AJNR American Journal of Neuroradiology* 2008;29:198-203.
10. Owler BK, Momjian S, Czosnyka Z, et al. Normal pressure hydrocephalus and cerebral blood flow: a PET study of baseline values. *Journal of Cerebral Blood Flow and Metabolism* 2004;24:17-23.
11. Scheltens P, van de Pol L. Impact commentaries. Atrophy of medial temporal lobes on MRI in "probable" Alzheimer's disease and normal ageing: diagnostic value and neuropsychological correlates. *Journal of Neurology, Neurosurgery, and Psychiatry* 2012;83:1038-40.
12. Barnes LL, Schneider JA, Boyle PA, Bienias JL, Bennett DA. Memory complaints are related to Alzheimer disease pathology in older persons. *Neurology* 2006;67:1581-5.

2

MMSE scores correlate with local ventricular enlargement in the spectrum from cognitively normal to Alzheimer's disease

NeuroImage. 2008;39(4):1832-8

L. Ferrarini
W.M. Palm
H. Olofsen
R. van der Landen
G.J. Blauw
R.G. Westendorp
E.L.E.M. Bollen
H.A.M. Middelkoop
J.H. Reiber
M.A. van Buchem
F. Admiraal-Behloul

Abstract

In this work, we aimed at correlating focal atrophy in periventricular structures with cognitive function, in the spectrum from healthy subjects to severe Alzheimer's disease: 28 subjects with normal cognition and 84 patients presenting various degrees of cognitive impairment were included in the study. The cognitive level of each subject was assessed with the Mini-Mental State Examination (MMSE). Atrophy in periventricular structures was inferred by modeling and analyzing local shape variations of brain ventricles: for a given subject, we distinguished between the severity of atrophy, estimated as local enlargement (in mm) of the ventricular surface relative to an average normal subject, and the extent of atrophy, defined as the percentage of the ventricular surface (global or per anatomical region) significantly different from an average control. Linear regression across subjects was performed to evaluate the correlation between atrophy and MMSE score. The severity of atrophy showed good correlation with MMSE score in the left thalamus, the left temporal horn, the left corona radiata, and the right caudate nucleus. The extent of atrophy showed no significant correlations. In conclusion, the MMSE scores correlate with localized depth of atrophy in well-defined periventricular structures.

Introduction

Dementia is usually defined as a progressive decline of cognitive function. Among the several possible causes of dementia, Alzheimer's disease (AD) is usually regarded as the most common one. Considering the spectrum of cognitive function, healthy subjects are at one end, presenting normal cognitive level, while patients with severe Alzheimer's disease (AD) are at the very opposite side. An important intermediate position is represented by mild cognitive impairment (MCI): patients suffering of MCI experience isolated memory deficits (amnesia), but are otherwise cognitively capable and not limited in their daily life. Growing evidence of how AD affects brain structures has previously been presented: hippocampal atrophy;¹⁻⁵ rapid degeneration of prefrontal lobe;^{6,7} atrophy of entorhinal cortex;⁸⁻¹¹ pronounced atrophy of the corpus callosum.¹²⁻¹⁴ Similar studies have analyzed the effects of MCI and its relationship with AD.¹⁵⁻¹⁷

Several cognitive tests exist to assess the cognitive level of an individual. One of them, the Mini-Mental State Examination (MMSE),¹⁸ has largely been used in clinical practice for the diagnostic work up of AD and MCI. Conspicuous attempts to correlate MMSE scores with brain structural changes, as captured by magnetic resonance imaging (MRI), have recently been reported in the literature: Thompson et al.¹⁹ showed high correlation in AD between MMSE scores and changes in temporal horns; Duan et al.²⁰ showed high correlation between cognitive impairment and selective white matter damage in AD, measured as a reduction of fractional anisotropy, particularly in the splenium of the corpus callosum; Apostolova et al.¹⁵ investigated the correlation between MMSE scores and hippocampal volume changes, finding no significant correlation in MCI-converters (among the subjects affected by MCI, some convert in time into AD and are referred to as MCI converters); Baxter et al.²¹ showed high correlation in AD between MMSE scores and decrease of gray matter in the left temporal lobe; finally, a strong correlation between MMSE scores and gray matter loss in several cortical regions was observed in clinical and pre-clinical AD.²²

The aim of our study was to investigate to what extent the MMSE score correlates with atrophy in periventricular structures. Any change in volume or shape in these structures must be reflected on the shape and volume of the brain ventricles: thus, by analyzing shape variations in the entire ventricular system we could indirectly estimate the degree of atrophy in all the periventricular structures. The delineation of small gray and white matter structures is a challenging task, particularly in elderly subjects, due to the loss of contrast between different tissues:²³ (semi-)automatic segmentation is error prone and not always reproducible, while manual delineation is highly time consuming. Cerebrospinal fluid (CSF), on the other hand, can be automatically and reliably

segmented, thanks to its sharp contrast with respect to the rest of the parenchyma. While analyzing atrophy, we introduced a distinction between the severity of atrophy and the extent of atrophy. The former was estimated as local enlargement (in mm) of the ventricular surface with respect to a normal average case; the latter was given by the percentage of ventricular surface significantly different from an average normal case. Finally, rather than focusing on only one specific pathological condition, such as AD or MCI, we included subjects from both groups, covering a larger area in the spectrum of cognitive impairment.

Materials and Methods

Subjects

The subjects included in the study were chosen so that a large area in the spectrum of cognitive function could be represented: 28 volunteers with normal cognitive function, and 84 patients presenting different degrees of cognitive impairment (26 subjects with MCI and 58 patients affected by AD, ranging from mild to severe cases). The volunteers were recruited through advertisements in local newspapers, while patients with cognitive impairment were consecutively referred to our outpatient memory clinic. The cognitive status was evaluated for all subjects using a standardized dementia screening, including a detailed medical history, a general internal and neurological exam, laboratory tests, neuropsychological testing (i.e., MMSE), and magnetic resonance images of the brain. Diagnoses were made in a multidisciplinary consensus meeting, according to the National Institute of Neurological and Communicative Disorders and Stroke–Alzheimer's Disease and Related Disorders Association (NINCDS-ADRDA) criteria for probable AD, and the Petersen criteria for MCI. Table 3.1 shows the demographic data: t tests performed on age and sex showed no significant difference between groups ($p < 0.01$). Subjects were included if they were older than 60 years, had no other neurologic or psychiatric illness, and had no abnormalities on MRI other than white matter hyperintensities or an incidental small lacunar lesion (≤ 5 -mm diameter). Approval by the local Medical Ethical Committee was granted to the study. Written informed consent was obtained from all subjects or from a close relative if a patient was demented.

Table 3.1 Demographic data: total number of subjects per group (and total number of male), age (in years), and MMSE score

	Controls	Patients
Tot (<i>N</i> male)	28 (12)	84 (38)
Age μ (σ)	74 (6.9)	74 (7.3)
MMSE μ (σ)	27.6 (1.7)	20.8 (5.6)
	[min–max]	[4–30]

MRI acquisition and image pre-processing

Magnetic resonance images were acquired on a 1.5-T MR-system (Philips Medical Systems, Best, The Netherlands) using the following pulse sequences: dual fast spin-echo (proton density and T2 weighted): time to echo (TE) 27/120 ms, repetition time (TR) 3000 ms, 48 contiguous 3-mm slices without an interslice gap, matrix 256 × 256, field of view (FOV) 220 mm; FLAIR (fluid attenuated inversion recovery): TE 100 ms, TR 8000, 48 contiguous 3-mm slices without an interslice gap, matrix 256 × 256, FOV 220 mm.

Images were pre-processed with our in-house developed automatic segmentation software,²⁴ which automatically extracted the intracranial cavity, the CSF, and the white matter hyperintensities. Three-dimensional region growing was applied to re-label the ventricular CSF as ventricles. Automatic affine 12-parameter image registration,²⁵ was applied to normalize all the images and the ventricular segmentations to the LUMC T2-weighted brain template for geriatrics,²⁶ in order to correct for brain size and orientation.

Shape modeling

The measure of focal atrophy in periventricular structures is based on the corresponding deformations occurring in the shape of the brain ventricles. Thus, as a first step one needs to model all the brain ventricles with comparable meshes. This was done with an automatic modeling technique previously introduced in Ferrarini et al.²⁷ the healthy subjects are used to generate an average brain ventricle image, whose surface is modeled by a growing and adapting mesh (see Fig. 3.1 (top)); subsequently, the mesh's structure is frozen (nodes are not added nor removed), and the mesh's shape is automatically adapted to all the ventricles in the study, ending up with comparable meshes (i.e., each node in a given mesh is uniquely associated with corresponding nodes in the other meshes). Local changes in ventricular shapes should be associated with focal atrophy in periventricular structures: thus, an expert was asked to manually delineate several regions on the initial average ventricular volume, each

corresponding to an adjacent periventricular structure. Nodes in the first mesh were then labeled accordingly to the closest region (see Fig. 3.1 (bottom)), and labels were propagated to all the other meshes. We visually inspected the results across all the meshes, to guarantee correct correspondence between labels and adjacent periventricular structures. In the remaining of this paper, the terms region left (right) corona radiata, region left (right) caudate nuclei, etc., will refer to the sets of nodes associated with the corresponding periventricular structures.

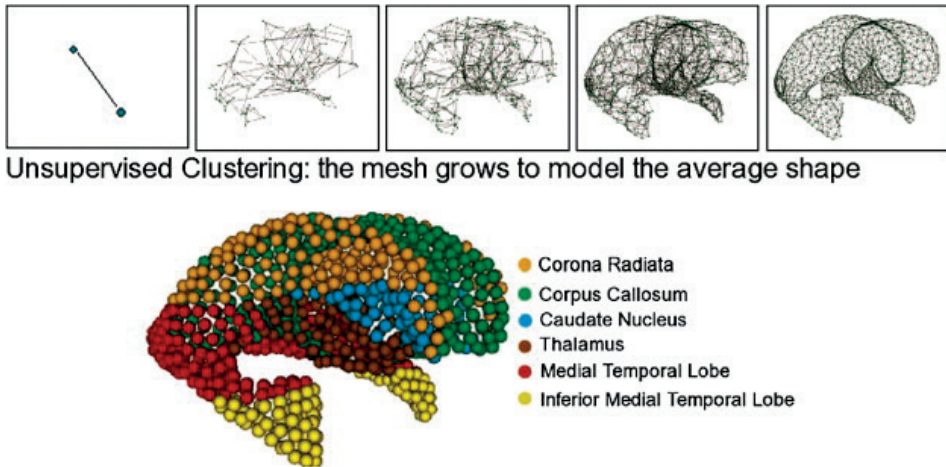


Figure 3.1

(Top) Shape modeling of an average ventricle: a mesh grows and adapts to model an average control surface. (Bottom) The ventricle volume was manually divided in regions, according to the adjacent periventricular structures, and each node was labeled accordingly.

Pre-statistical shape analysis

Does MMSE score correlate with severity of focal atrophy?

We have assessed the significance of the correlation between the severity of focal atrophy and MMSE score for each location (i.e., node) on the ventricular surface. Considering a particular node in a given subject, one can evaluate its Euclidian distance in space to the corresponding node in the average mesh, obtained from the control group. The underlying idea is that focal atrophy in periventricular structures should lead to a more pronounced local ventricular enlargement, and subsequently to larger distances between a given node and the corresponding one in the average control. We visually checked that all the non-control ventricles presented larger structures than the average control. For each node, the local enlargements across all subjects were correlated with the corresponding MMSE scores: the statistical analysis and the results are reported in the MMSE correlation with severity of atrophy section.

Does MMSE score correlate with the extent of atrophy?

A similar approach was taken to evaluate the correlation between the MMSE score and the extent of atrophy. Starting with the average mesh previously introduced, for each node i we modeled the local distribution in space of the control population, evaluating the average distance μ_i and the standard deviation σ_i (with $i = 1, 2, \dots, N_{\text{Nodes}}$) (see Fig. 3.2). Subsequently, considering a subject j , for each node i we evaluated its Euclidian distance d_i^j to the corresponding node in the average mesh. The location i in subject j was then labeled as:

$$l_i^j = \begin{cases} 1 & \text{if } d_i^j > \mu_i + 3\sigma_i \\ 0 & \text{otherwise} \end{cases}$$

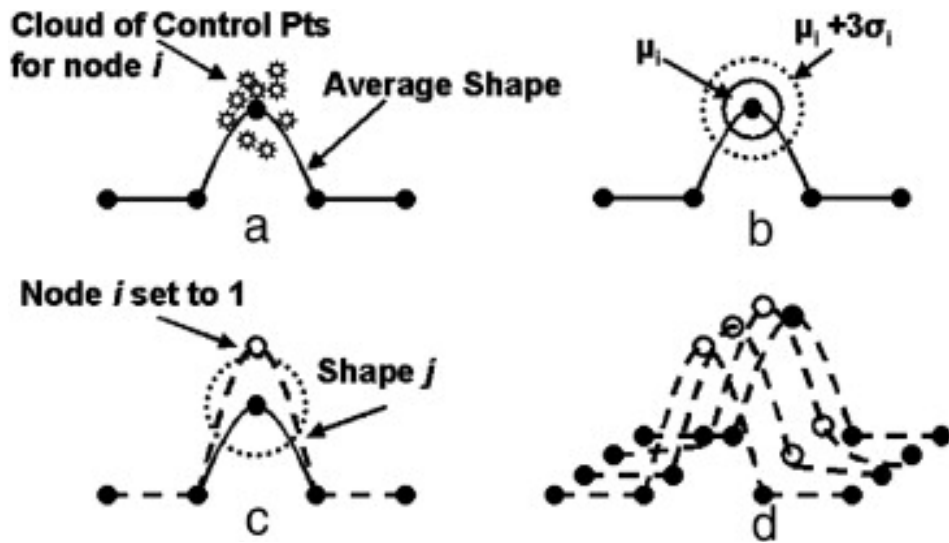


Figure 3.2

Extent of atrophy measurement. (a) Spatial distribution of the control population around node i of the average shape. (b) Average distance μ_i and threshold $\mu_i + 3\sigma_i$. (c) In a shape j , the node i is labeled as 1 if its distance from the average node is higher than the threshold. (d) The extent of atrophy is the percentage of nodes set to 1.

For each subject and for each region, we could therefore evaluate the percentage of locations set to 1, corresponding to the local extent of atrophy. Such values were finally correlated, across all subjects, with the MMSE scores: permutation tests were used to assess the significance level (p-value) of the correlation. Results are reported in the MMSE correlation with extent of atrophy section.

Results

MMSE correlation with severity of atrophy

For each given node, we performed a linear regression correlating local distances of all subjects from the control average node, to the MMSE scores associated with the subjects. The statistical significance of the correlation was assessed via permutation tests, correcting for multiple comparisons. Thus, the results provided us, for each node, with a p-value indicating the significance of the correlation in that particular location. Mapping the p-values on an average control, we could visually highlight areas with higher correlation (see Fig. 3.3). Results were then clustered into the manually delineated regions, and for each region we evaluated the percentage of surface in which the severity of atrophy significantly correlated with the MMSE score: this made it possible to identify the regions (and, consequently, the periventricular structures) with higher correlation. Fig. 3.4 shows the percentage of area in which the severity of atrophy correlates ($p < 0.05$) with the MMSE score, for each manually delineated region (the whole, left, and right ventricular systems are also considered). Some regions show a high correlation: left corona radiata, right caudate nucleus, left caudate nucleus, left thalamus, and left medial temporal horn. Other regions, on the other hand, are almost completely uncorrelated: right side of the corpus callosum, right side of the thalamus, left inferior medial temporal horn. It is notable that the severity of atrophy in left periventricular structures (reflected in the left ventricular system) presents a higher correlation with the MMSE score than those on the right.

MMSE correlation with extent of atrophy

We performed a linear regression analysis to correlate the MMSE score and the extent of atrophy for the whole, left, and right ventricular systems, as well as for each of the manually delineated regions. All subjects were included in the analysis, and both the R^2 statistic and the corresponding p-value were evaluated. Results are reported in Table 3.2. No significant correlation was found in any of the analyzed areas. Only in the left inferior medial temporal horn we could detect a trend, showing that higher MMSE scores reflect smaller extents of atrophy: nevertheless, the correlation was not significant (p-value = 0.06). The results were not corrected for multiple comparison: even without correction, no significant correlation was detected, supporting the idea that no correlation exists between extent of atrophy and MMSE scores.

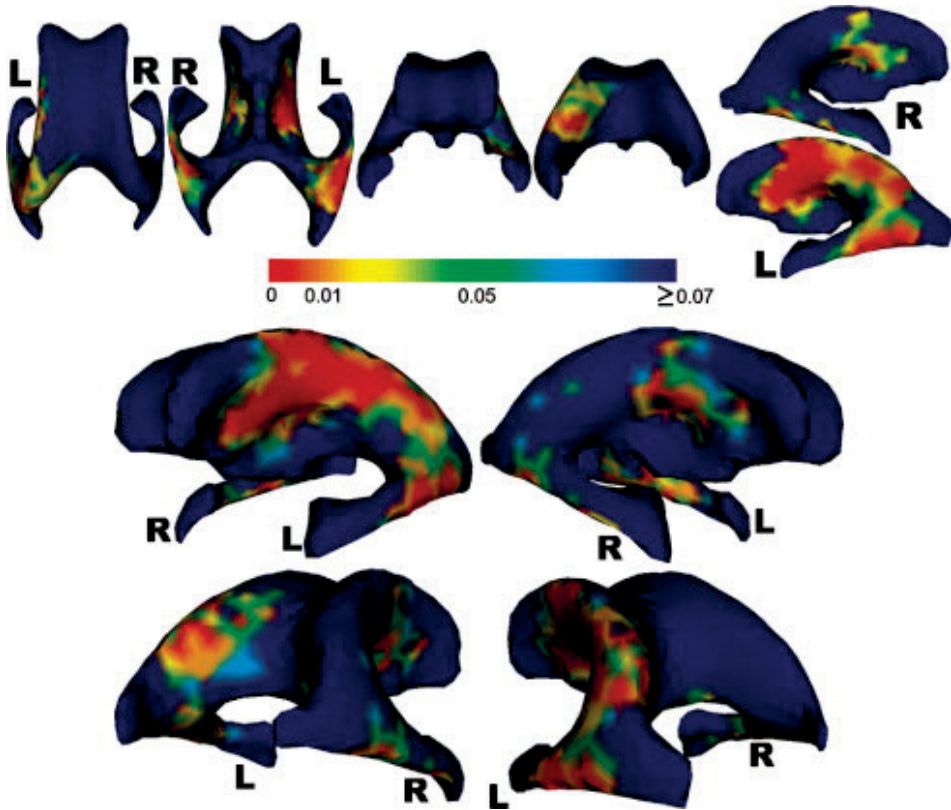


Figure 3.3
Local correlation between severity of atrophy and cognitive impairment, across all subjects (controls and patients). Orthogonal (top) and prospective (bottom) views (p-values higher than 0.05 are plotted in blue).

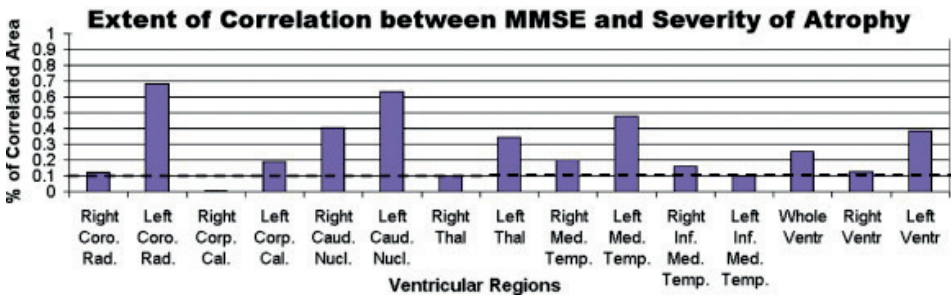


Figure 3.4
Extent of correlation for the severity of atrophy. For each region, we plot the percentage of ventricular surface whose severity of atrophy (see Fig. 3.3) significantly correlates with the MMSE score.

Table 3.2 Linear regression between extent of atrophy and MMSE score (all 112 subjects included): for each area, we report the R^2 value and the corresponding p value. No significant correlation was found (p threshold set at 0.05).

		R^2	p -Value
Whole ventricle		0.01	0.67
Right ventricle		10^{-6}	1.00
Left ventricle		0.03	0.40
Corona radiata	R	0.01	0.66
	L	0.01	0.75
Corpus callosum	R	0.03	0.39
	L	0.01	0.70
Caudate nuclei	R	0.03	0.39
	L	0.03	0.43
Thalamus	R	0.001	0.88
	L	10^{-4}	0.94
Superior medial temporal horn	R	10^{-4}	0.92
	L	0.05	0.31
Inferior medial temporal horn	R	0.003	0.78
	L	0.14	0.06

Discussion and conclusions

In this work, we have investigated the correlation between atrophy in periventricular structures and cognitive function, in the spectrum from normal cognition to severe AD. The analysis of structural changes in periventricular structures always presents some serious challenges. First, one should choose between volumetric or shape-based analyses. In Van der Flier et al.,²⁸ the authors analyzed a subset of the population used in this study, showing that MR volumetric measurements of the brain correlate with cognitive decline in non-demented elderly. The volume changes, being inherently global, are less subject to small segmentation errors; shape-based methods, on the other hand, aiming at a localized analysis, are more sensitive to the accuracy of the segmentation. Conversely, the volumetric distributions of periventricular structures in normal and non-normal populations might overlap and fail to provide discriminative results; shape analysis, highlighting more localized differences, is less keen to this problem. Thus, a shape analysis of periventricular structures is to be preferred. Unfortunately, the intensity contrast between white and gray matter decreases with age,²³ making it a more difficult and less accurate task to delineate periventricular

structures in MR. On the other hand, the contrast between CSF and the remaining parenchyma stays sharp in elderly, allowing automatic tools to reliably segment ventricular CSF. In our study, we have analyzed shape changes of the whole ventricular system as an indirect tool to investigate atrophy in the surrounding periventricular structures: this differs from previous methods which focused more on singular gray/white matter structures or specific ventricular areas.^{15,19-20} Moreover, we introduced a clear separation between severity of atrophy and extent of atrophy, showing that the former correlates with cognitive impairment, while the second does not: while doing this, we explored a large area in the spectrum of cognitive function, including both subjects with MCI and AD, while previous methods focused more on AD,¹⁹⁻²⁰ on AD and a limited number of converting MCI,²² or on converting and non-converting MCI.¹⁵

The assessment of a subject's cognitive function is not a trivial task. In this work, we have chosen to use the MMSE score as an estimation of an individual's cognitive level. This choice was justified by the fact that, despite its limitations, the MMSE score is largely used in the diagnostic work up of AD and MCI in clinical routine. Thus, a better understanding of how the MMSE score relates to periventricular atrophy is important. Global measurements of brain atrophy have already been proved to correlate with MMSE scores.²⁹⁻³⁰ The local analysis presented in this work aimed at further improving our knowledge on how damage in specific periventricular structures contributes to the assessment of an individual's cognitive level.

The results lead to some further considerations. The severity of cognitive impairment seems to correlate significantly with increased severity of atrophy in well-defined periventricular structures. More specifically, areas like the left corona radiata, right and left caudate nuclei, left side of the thalamus, left medial temporal horn, and the left side of the splenium in the corpus callosum showed high correlation between severity of atrophy and cognitive impairment. These findings are in agreement with those previously reported in the literature: a correlation between dementia and infarcts in the left corona radiata was highlighted in Pohjasvaara et al.³¹ the left temporal horn and its correlation with dementia is well-established,¹⁵ Thompson et al.,¹⁹ and shows how atrophy of the temporal lobe and hippocampus is inherently related with the disease; involvement of the left side of the splenium in the corpus callosum was highlighted by Duan et al.,²⁰ by using global diffusion tensor images for healthy subjects and ADs. Thompson et al.¹⁹ suggested that a lack of correlation between cognitive decline and hippocampal atrophy might be due to the MMSE test itself, since it is mostly related with cortical functions. Our findings on the thalamus might lead to some further considerations: the thalamus is responsible to code and transmit information to the

cortex, particularly for what concerns the sensory system (auditory system, visual system, etc.): thus, impairments of cortical functions might also occur as a consequence of thalamus deficits. Finally, looking at the whole, left, and right ventricular systems, it is clear that the severity of atrophy in the left hemisphere presents a higher correlation. This result is consistent with previous studies showing how changes in left periventricular structures relate to MCI and AD: particularly Scher et al.³² showed consistent patterns of shape differences in AD in the body of the left hippocampus; Whitwell et al.³³ showed gray matter loss in the left anterior inferior temporal lobe in nonamnestic MCI; Yavuz et al.³⁴ correlated MMSE scores with volume loss of both left and right hippocampi; finally Müller et al.³⁵ showed that the left hippocampus volume is an accurate diagnostic variable for MCI. When we tried to correlate the extent of atrophy with cognitive function, we could not find any significant result. The only exception was the left inferior medial temporal horn, which presented an almost significant correlation ($p = 0.06$).

The assumption that MMSE scores can confidently reflect cognitive impairment is open to discussion. Neuropsychological tests usually provide a large set of indicators to estimate the cognitive level of an individual. The MMSE test is a global composite measurement of different cognitive functions, spatially located in different parts of the brain. Some criticisms have been moved to the use of MMSE test, especially when assessing the cognitive level of healthy subjects or patients with MCI. Nevertheless, the MMSE test keeps being intensively used in the diagnosis of AD and MCI: thus, efforts to improve our understanding on its relation with brain structural changes are largely justified. To the best of our knowledge, this is the first study which clearly distinguishes between different kinds of atrophy in periventricular structures and correlates them with cognitive impairment in MCI and AD, as estimated by the MMSE score.

In conclusion, our results suggest that worse MMSE scores correlate with an increased severity of atrophy in well-defined periventricular structures. Future research might focus on other global tests, such as the Camcog, and more specific cognitive tests: a comparison between tests could strength even further the link between cognitive impairment and atrophy of well-defined periventricular structures.

Acknowledgments

This work was supported by the Technology Foundation STW (project number LNN. 6122), and by Medis medical imaging systems BV, Leiden, The Netherlands (<http://www.medis.nl>).

References

1. Freeborough, P., Fox, N., 1997. The boundary shift integral: an accurate measure of cerebral volume changes from registered repeat MRI. *IEEE Transactions on Medical Imaging*. 16 (5), 623–629.
2. Pitiot, A., Delingette, H., Toga, A., Thompson, P., 2003. Learning object correspondences with the observed transport shape measure. *Information Processing in Medical Imaging, IPMI* 25–37.
3. Rueckert, D., Frangi, A., Schnabel, J., 2003. Automatic construction of 3-D statistical deformation models of the brain using nonrigid registration. *IEEE Transactions in Medical Imaging*. 22 (8), 1014–1025.
4. Schott, J., Price, S., Frost, C., Whitwell, J., Rossor, M., Fox, N., 2005. Measuring atrophy in Alzheimer diseases: a serial MRI study over 6 and 12 months. *Neurology* 65, 119–124.
5. Thodberg, H., 2003. Minimum description length shape and appearance models. *Information Processing in Medical Imaging, IPMI* 51–62.
6. Coffey, C., Wilkinson, W., Parashos, I., 1992. Quantitative cerebral anatomy of aging human brain: a cross-sectional study using magnetic resonance imaging. *Neurology* 42, 527–536.
7. Raz, N., Gunning, F., Head, D., 1997. Selective aging of the human cerebral cortex observed in vivo: differential vulnerability of the prefrontal gray matter. *Cerebral Cortex* 7, 268–282.
8. Barns, J., Scahill, R., Boyes, R., Frost, C., Lewis, E., Rossor, C., Rossor, M., Fox, N., 2004. Differentiating ad from aging using semiautomated measurement of hippocampal atrophy rates. *NeuroImage* 23,574–581.
9. Dekaban, A., 1978. Changes in brain weights during the span of human life: relation of brain weights to body heights and body weights. *Annals of Neurology* 4, 345–356.
10. Lerch, J., Priesner, J., Zijdenbos, A., Hamperl, H., Teipel, S., Evans, A., 2004. Focal decline of cortical thickness in Alzheimer’s disease identified by computational neuroanatomy. *Cerebral Cortex* 15, 995–1001.
11. Pruessner, J., Collins, D., Pruessner, M., Evans, A., 2001. Age and gender predict volume decline in the anterior and posterior hippocampus in early adulthood. *Journal of Neuroscience*. 21 (1), 194–200.
12. Bozzao, A., Floris, R., Baviera, M., Apruzzese, A., Simonetti, G., 2001. Diffusion and perfusion MR imaging in cases of Alzheimer’s disease: correlations with cortical atrophy and lesion load. *AJNR American Journal of Neuroradiology*. 22, 1030–1036.
13. Hanyu, H., Asano, T., Sakurai, H., Imon, Y., Takazaki, M., Shindo, H., Abe, K., 1999. Diffusion-weighted and magnetization transfer imaging of the corpus callosum in Alzheimer’s disease: a quantitative study. *Journal of the Neurological Sciences* 167, 37–44.
14. Teipel, S., Bayer, W., Alexander, G., Zebhuhr, Y., Teichberg, D., Kulic, L., Schapiro, M., Moller, H., Rapoport, S., Hampel, H., 2002. Progression of corpus callosum atrophy in Alzheimer disease. *Archives of Neurology* 59,243–248.
15. Apostolova, L., Dutton, R., Dinov, I., Hayashi, K., Toga, A., Cummings, J., Thompson, P., 2006. Conversion of mild cognitive impairment to Alzheimer disease predicted by hippocampal atrophy maps. *Archives of Neurology* 63, 693– 699.
16. Carmichael, O., Thompson, P., Dutton, R., Lu, A., Lee, S., Lee, J., Kuller, L., Lopez, O., Aizenstein, H., Meltzer, C., Liu, Y., Toga, A., Becker, J., 2006. Mapping ventricular changes related to dementia and mild cognitive impairment in a large community-based cohort. *ISBI* 315–318.
17. Chételat, G., Landeau, B., Mezenge, F., Viader, F., de la Sayette, V., Desgranges, B., Baron, J., 2005. Using voxel-based morphometry to map structural changes associated with rapid conversion in MCI: a longitudinal MRI study. *NeuroImage* 27, 934–946.
18. Folstein, M., Folstein, S., McHugh, P., 1975. Mini-mental state. *Journal of Psychiatric Research* 12, 189–198.

19. Thompson, P., Hayashi, K., de Zubicaray, G., Janke, A., Rose, S., Semple, J., Hong, M., Herman, D., Gravano, D., Doddrell, D., Toga, A., 2004. Mapping hippocampal and ventricular change in Alzheimer disease. *NeuroImage* 22 (4), 1754–1766.
20. Duan, J., Wang, H., Xu, J., Lin, X., Chen, S., Kang, Z., Yao, Z., 2006. White matter damage of patients with Alzheimer's disease correlated with the disease cognitive function. *Surgical and Radiologic Anatomy* 28, 150–156.
21. Baxter, L., Sparks, D., Johnson, S., Lenoski, B., Lopez, J., Connor, D., Sabbagh, M., 2006. Relationship of cognitive measures and gray and white matter in Alzheimer's disease. *Journal of Alzheimer's Disease*. 9 (3), 253–260.
22. Apostolova, L., Lu, P., Dutton, R., Hayashi, K., Toga, A., Cummings, J., Thompson, P., 2006. 3D mapping of Mini-Mental State Examination performances in clinical and preclinical Alzheimer disease. *Alzheimer Disease and Associated Disorders* 20 (4), 224–231.
23. Magnaldi, S., Ulkmar, M., Vasciaveo, A., Longo, R., Pozzi-Mucelli, R.S., 1993. Contrast between white and grey matter: MRI appearance with aging. *European Radiology* 3 (6), 513–519.
24. Admiraal-Behloul, F., van den Heuvel, D., Olofsen, H., van Osch, M., 2005. Fully automatic segmentation of white matter hyperintensities in MR images of the elderly. *NeuroImage* 28 (3), 607–617.
25. Woods, R., Grafton, S., Holmes, C., Chery, S., Mazziotta, J., 1998. Automated image registration: I. general methods and intrasubject, intramodality validation. *Journal of Computer Assisted Tomography* 22, 139–152.
26. Admiraal-Behloul, F., van den Heuvel, D., Olofsen, H., Schmitz, N., van Buchem, M.A., 2003. Brain templates for the elderly. *Proceedings of the International Society for Magnetic Resonance in Medicine (ISMRM)*, Toronto.
27. Ferrarini, L., Olofsen, H., Palm, W., van Buchem, M., Reiber, J., Admiraal-Behloul, F., 2007. Games: growing and adaptive meshes for fully automatic shape modeling and analysis. *Medical Image Analysis* 11 (3), 302–314.
28. Van der Flier, W.M., van der Vlies, A.E., Wervelings, A.W.E., de Boer, N.L., Admiraal-Behloul, F., Bollen, E.L.E.M., Westendorp, R.G.J., van Buchem, M.A., Middelkoop, H.A.M., 2005. MRI measures and progression of cognitive decline in nondemented elderly attending memory clinic. *International Journal of Geriatric Psychiatry* 20 (11), 1060–1066.
29. Fox, N.C., Scahill, R.I., Crum, W.R., Rossor, M.N., 1999. Correlation between rates of brain atrophy and cognitive decline in AD. *Neurology* 52 (8), 1687–1688.
30. Duarte, A., Hayasaka, S., Du, A., Schuff, N., Jahng, G., Kramer, J., Miller, B., Weiner, M., 2006. Volumetric correlates of memory and executive function in normal elderly, mild cognitive impairment and Alzheimer's Disease. *Neuroscience Letters* 406 (1-2), 60–65.
31. Pohjasvaara, T., Mantyla, R., Salonen, O., Aronen, H., Ylikoski, R., Hietanem, M., Kaste, M., Erkinjuntti, T., 2000. MRI correlates of dementia after first clinical ischemic stroke. *Journal of Neurological Sciences*. 181 (1-2), 111–117.
32. Scher, A.I., Xu, Y., Korf, E.S., White, L.R., Scheltens, P., Toga, A.W., Thompson, P.M., Hartley, S.W., Witter, M.P., Valentino, D.J., Launer, L.J., 2007. Hippocampal shape analysis in Alzheimer's disease: a population-based study. *NeuroImage* 36 (1), 8–18.
33. Whitwell, J.L., Petersen, R.C., Neqash, S., Weiqand, S.D., Kantarci, K., Ivnik, R.J., Knopman, D.S., Boeve, B.F., Smith, G.E., Jack Jr., C.R., 2007. Patterns of atrophy differ among specific subtypes of mild cognitive impairment. *Archives of Neurology* 64 (8), 1130–1138.
34. Yavuz, B.B., Arioqul, S., Cankurtaran, M., Oquz, K.K., Halil, M., Daqli, N., Cankurtaran, E.S., 2007. Hippocampal atrophy correlates with the severity of cognitive decline. *International Psychogeriatrics* 19 (4), 767–777.
35. Müller, M.J., Greverus, D., Weibrich, C., Dellani, P.R., Scheurich, A., Stoeter, P., Fellgiebel, A., 2007. Diagnostic utility of hippocampal size and mean diffusivity in amnesic MCI. *Neurobiology of Aging* 28 (3), 398–403.

3

Cerebral atrophy in elderly with subjective memory complaints

Journal of Magnetic Resonance Imaging.
2013;38(2):358-64

W.M. Palm
L. Ferrarini
W.M. van der Flier
R.G. Westendorp
E.L.E.M. Bollen
H.A.M. Middelkoop
J.R. Milles
J. van der Grond
M.A. van Buchem

Abstract

To evaluate ventricular shape differences along the complete surface of the lateral and third ventricles of persons with subjective memory complaints (MC).

We included 28 controls and 21 persons with MC. FLAIR, T2 and PD-weighted brain MRI scans were acquired at 1.5 T, followed by semi-automated segmentation of the lateral and third ventricles, and local shape difference analysis based on growing and adaptive meshes. Ventricular meshes were used to highlight local areas with significant differences between controls and persons with MC, determined by permutation tests with a predefined threshold ($p = 0.01$).

Compared to control subjects, relevant differences were found in the shape of the ventricular surface adjacent to the thalamus and corona radiata in persons with MC. Before correction for multiple comparisons, relevant differences were also found in the shape of the ventricular surface adjacent to the corpus callosum, hippocampus and amygdala.

Our findings suggest the presence of localized structural brain differences in patients with subjective memory complaints in the thalamus and the corona radiata.

Introduction

Subjective memory complaints are common in the elderly.¹ They are considered to be part of the spectrum that ranges from normal cognition to dementia.² Memory complaints are a core feature of Mild Cognitive Impairment (MCI), but in MCI these complaints can be verified with cognitive testing.³ However, a fair number of elderly have memory complaints that cannot be substantiated with formal cognitive testing. The presence of subjective memory complaints significantly increases the risk of future cognitive decline,⁴ however, not as significant as in MCI, which leads to dementia in about half the cases.³ Furthermore, Alzheimer's disease (AD) pathology has been observed in persons with subjective memory complaints on post-mortem examination, including amyloid plaques and neurofibrillary tangles.⁵ It has been suggested that memory complaints in older persons may indicate self-awareness of a degenerative pathologic process.⁵

Using segmentation techniques on MR images, atrophy has been detected in persons with subjective memory complaints in two specific regions of the brain: the corpus callosum (6) and hippocampus.⁷⁻⁹ Segmentation of these structures is relatively simple, since a large part of these structures is surrounded by CSF, offering a sharp contrast that increases the reliability of segmentation techniques. However, segmentation of other brain structures that are not surrounded by CSF is more challenging since the borders of these structures are less clear. Furthermore, due to the aging process, such borders may fade away, further complicating segmentation. The border between the cortical gray and subcortical white matter in particular is known to lose contrast with aging. Lack of reliable tools to segment the basal ganglia and thalamus is one of the reasons why involvement of these structures in subjective memory complaints has not been assessed thus far.

The shape of the cerebral ventricles may be analyzed as an indirect measure of cerebral atrophy. Since atrophy of periventricular structures results in compensatory changes (local dilatation) in ventricular shape, this method offers a reliable way to detect atrophy in periventricular structures. The advantage of this technique is that it relies on the high contrast border between ventricles and brain parenchyma. This method has been validated¹⁰ and applied in patients. In patients with AD, it detected shape differences on the ventricular surface of the medial temporal horn, the corpus callosum, the thalamus and the caudate nucleus.¹¹

In the present, explorative study we compare the ventricular shapes of persons with subjective memory complaints to those of control subjects. Our aim is to search for

localized shape differences in the complete ventricular surface of persons with subjective memory complaints, as an indirect measure of regional atrophy in adjacent periventricular gray matter structures.

Materials and Methods

Subjects

Twenty-one consecutive self-referred persons with subjective memory complaints from the outpatient memory clinic of our institution participated in this study. The diagnosis of subjective memory complaints was made in the absence of abnormalities in neuropsychological test results, according to age and educational level. Twenty-eight elderly controls without memory complaints were recruited through an advertisement in a local newspaper. The study was approved by the institutional review board. Written informed consent was obtained from all persons. Table 4.1 shows the demographic data of our study sample. Controls did not differ from memory complainers in age (Independent Samples T-test, $p = 0.08$) or gender (Fisher's Exact Test, $p = 0.56$).

Table 4.1 Demographics and Neuropsychological Assessment

	Controls	Subjective MC	P-value
Total	28	21	
Males, percentage	12, 43%	7, 33%	0.56
Age, mean	74.1 (6.9)	70.4 (7.3)	0.08
CAMCOG, total score	95.9 (4.2)	93.8 (5.5)	0.12
MMSE	27.6 (1.7)	28.2 (1.7)	0.20
WMS, memory quotient	126.9 (11.9)	119.9 (16.0)	0.07
ADAS, total good score	19.2 (3.5)	18.1 (3.9)	0.31
Boston, score	25.4 (3.3)	25.0 (3.4)	0.67
FAS, good score	35.0 (12.1)	34.3 (10.3)	0.83
Benton, good score	5.2 (1.6)	5.4 (2.0)	0.71
TMT part A, time in seconds	33.5 (11.3)	51.8 (22.7)	< 0.001
TMT part B, time in seconds	83.1 (32.6)	129.4 (54.6)	0.001
WAIS-R substitution, rough score	42.2 (8.7)	35.5 (9.0)	0.01

Standard deviations are presented in brackets. MC = Memory Complaints; CAMCOG = Cambridge Cognitive Examination; MMSE = Mini-Mental State Examination; WMS = Wechsler Memory Scale; ADAS = Alzheimer's Disease Assessment Scale; FAS = Letter Fluency; TMT = Trail Making Test; WAIS = Wechsler Adult Intelligence Scale-Revised.

Neuropsychological assessment

All participants were subject to a standardized neuropsychological test battery. Global cognitive functioning was assessed using the Cambridge Cognitive Examination (CAMCOG) (12,13), which incorporates the Mini-Mental State Examination (MMSE).¹⁴ The CAMCOG provides a total score for global cognitive functioning as well as subscores for specific cognitive functions (memory, orientation, language, praxis, and gnosis). Memory was also evaluated using the Wechsler Memory Scale (WMS)¹⁵ and word recall from the Alzheimer's Disease Assessment Scale (ADAS)¹⁶. The Boston Naming Test¹⁷ was employed to yield an additional measure of language function. Tests of executive functioning included letter (FAS) and category (animals, jobs) fluency,¹⁸ the Trail Making Test (TMT)¹⁹ and the digit symbol subtest of the Wechsler Adult Intelligence Scale–Revised.²⁰ Neuropsychological test results were compared between controls and persons with subjective memory complaints using Independent Samples T-tests. Data from MMSE, WMS, Boston, TMT A and TMT B were skewed and were therefore first log-transformed. The TMT scores were significantly different, indicating a difference in executive functioning. However, our other neuropsychological tests showed no difference in memory and global cognitive performance. The diagnosis of memory complainer was made on the basis of a clinical assessment by the neuropsychological department of our institution. Overall, neuropsychological test results for memory complainers were within normal limits.

MRI acquisition and analysis

Magnetic resonance images were acquired on a 1.5-T MR-system (Philips Medical Systems, Best, The Netherlands) using a dual fast spin-echo (proton density and T2 weighted) sequence: time to echo (TE) 27 ms, repetition time (TR) 3000 ms, 48 contiguous 3-mm slices without an interslice gap, matrix 256 x 256, field of view (FOV) 220 mm. The line through the inferior border of the genu and splenium of the corpus callosum defined the direction of scanning. Segmentation was performed using SNIPER (Software for Neuro-Image Processing in Experimental Research),²¹ an in-house developed software program, consisting of automatic 3D registration, automatic segmentation of intra-cranial cavity and CSF volumes, followed by manual labeling of lateral and third ventricles on CSF masks with semi-automatic region growing, and calculation of volumes. All the images were then corrected for head-size and orientation using automatic affine 12-parameters registration to the LUMC T2-weighted brain template for geriatrics.^{21,22}

Ventricular meshes

Morphological analysis required, as a first step, the transformation of the brain ventricles into comparable ventricular meshes. This was performed following an

automatic procedure that has been described before.²³ An average shape was created from the control population. This involved several steps: first, a voxel-count map was built up by adding all controls' binary volumes; subsequently, a threshold was applied to the voxel-count map, obtaining an average control ventricle. GAMEs (Growing and Adaptive Meshes)¹⁰ was then applied to the average volume: initially, a mesh was grown (adding nodes and edges) until it converged to a good representation of the average control shape; once the first mesh was obtained, the number of nodes and edges was frozen. In a second phase the mesh was adapted to all the instances in the two populations using the Kohonen self-organizing map algorithm.²⁴ Since nodes were not added nor removed, all the final meshes were comparable: each node in a given mesh was uniquely associated with another node in another mesh, allowing for local comparison between meshes. Local shape difference analysis was based on such comparable meshes, in which corresponding nodes were representative of similar anatomical locations.

Ventricular surface parcellation

In order to quantify the extent of local shape differences in the different groups and relate it to particular periventricular structures, we manually parcellated the total ventricular surface into regions, according to the adjacent anatomical structures: the left and right corona radiata, the left and right side of the corpus callosum, the left and right caudate nuclei, the left and right thalamus, the left and right superior medial temporal horns and the left and right inferior medial temporal horns. This manual delineation was performed only once, using a regular anatomical atlas, on the template used to normalize all the brain images.²⁵ The parcellation procedure was performed by the first author (a resident physician in radiology) and second author (an information / software engineer), and verified by the last author (an experienced neuroradiologist). The software extracted fully automatically the intracranial cavity, the cerebrospinal fluid (CSF), and the white matter hyperintensities. The lateral and third ventricles were semiautomatically extracted by re-labeling the ventricular CSF to ventricles slice-by-slice, using interactive editing tools. The mesh's nodes were associated with the closest overlapping region, and clustered together in corresponding surface areas. The purpose of our manual delineation was to generate a meaningful regional parcellation of the ventricular surface, rather than to obtain an accurate delineation of the corresponding periventricular structures: such a parcellation allows a more detailed quantitative analysis of the differences between the groups.

Local shape difference analysis

Ventricular volume was not normally distributed in our study subjects (Lilliefors test for normal distribution). A non-parametric test (Mann-Whitney U) was used to compare median ventricular volume between the two groups.

Given two populations of brain ventricle meshes, permutation tests were applied at each node location to evaluate the significance of local shape differences: each location (i.e. node in the mesh) of the ventricles was associated with a p value, rendered with a color code on the ventricular surface, as shown in Figure 4.1. Locations with a p value below 0.01 were chosen as characteristic features for the brain ventricle's shapes. To prevent coincidental findings, significant differences were considered only when at least 1% of the nodes of a region proved significantly different. Displacement vectors were also evaluated at each location found to be significantly different: for our two groups of subjects, we generated two average meshes and evaluated the displacement in space between corresponding nodes. The direction of the displacement in the x, y and z directions was used to determine shrinkage (negative direction) or enlargement (positive direction) compared to controls. We found that the displacement was positive, indicating enlargement. Also, visual inspection of displacement vectors between controls and persons with subjective memory complaints showed that changes occurred as a result of enlargement of the ventricles in the group of subjects with subjective memory complaints. Ventricular shape differences between these groups were expressed as the percentage of nodes with significant displacement on the surface of a given structure, as well as the average displacement per area.

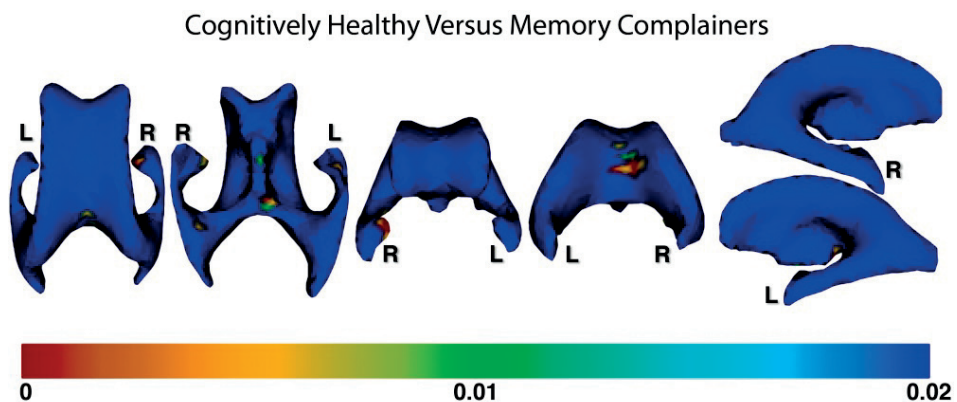


Figure 4.1 Ventricular shape comparison
Transverse, coronal and sagittal views of local differences in ventricular shape between controls and persons with subjective memory complaints. Uncorrected local shape differences between groups are represented by color-coded p-values.

Finally, a False Discovery Rate (FDR) correction was added to our local shape difference analysis, for which a p-value below 0.2 was chosen to evaluate differences between controls and persons with subjective memory complaints.

Results

Localized ventricular shape differences between persons with subjective memory complaints and controls, as well as the total number of nodes for each area, are presented in Table 4.2. This table shows uncorrected results ($P < 0.01$), as well as results after FDR correction ($P < 0.2$).

Table 4.2 Ventricular shape differences between controls and memory complainers

		Total number of nodes	P < 0.01 No FDR		FDR P < 0.2	
			%	mm	%	mm
Corona radiata	R	88	0	-	0	-
	L	91	0	-	1	2.2
Corpus callosum	R	140	5	1.8	0	-
	L	153	2	0.7	0	-
Caudate nucleus	R	32	0	-	0	-
	L	30	0	-	0	-
Thalamus	R	50	2	0.9	0	-
	L	38	3	0.4	8	2.2
Superior Medial Temporal Lobe	R	99	2	1.3	0	-
	L	122	0	-	0	-
Inferior Medial Temporal Lobe	R	55	13	1.1	0	-
	L	51	2	1.3	0	-

% = percentage of nodes on the surface of a given structure that show significant displacement; mm = average displacement per area in millimeters; FDR = False Discovery Rate.

Corpus callosum

Before FDR correction, relevant shape differences were found in the ventricular surface adjacent to the corpus callosum between persons with subjective memory complaints and controls. The right ventricular surface of the corpus callosum contained a larger percentage of different nodes (5%) than the left side (2%). In addition, average displacement was greater in the right ventricular surface of the corpus callosum (1.8

mm) than on the left (0.7 mm). After FDR correction, no nodes were found on the ventricular surface of the corpus callosum with significant displacement.

Inferior medial temporal horn

Before FDR correction, relevant shape differences were found in the ventricular surface of the inferior medial temporal horn between persons with subjective memory complaints and controls. The ventricular surface of the right inferior medial temporal horn contained a far larger percentage of different nodes (13%) than the ventricular surface of the left inferior medial temporal horn (2%). Average displacement was comparable between the ventricular surface of the right (1.1 mm) and left (1.3 mm) inferior medial temporal horns. After FDR correction, no nodes were found in the ventricular surface of the hippocampus with significant displacement.

Thalamus

Before FDR correction, relevant shape differences were found in the ventricular surface of the thalamus between persons with subjective memory complaints and controls. The ventricular surface of the left thalamus contained a larger percentage of different nodes (3%) than the ventricular surface of the right thalamus (2%). After FDR correction, 8% of the nodes in the ventricular surface of the left thalamus showed significant displacement, while no nodes with significant displacement were found in the ventricular surface of the right thalamus.

Corona radiata

Before FDR correction, no relevant shape differences were found between persons with subjective memory complaints and controls in the ventricular surface of the corona radiata. However, after FDR correction a single node (1% of the ventricular surface of the left corona radiata) showed significant displacement.

Remaining periventricular structures

For the ventricular surface of the superior medial temporal horn, a difference was only found on the right hemisphere (2% of nodes), which did not remain after FDR correction. Both before and after FDR correction, no relevant shape differences were found in the ventricular surface adjacent to the caudate nucleus.

Discussion

The main finding of our study is outward displacement of the ventricular surface adjacent to the thalamus and the corona radiata in persons with subjective memory

complaints, compared to controls. Uncorrected results showed tentative evidence of local shape differences in the ventricular surface of the corpus callosum, hippocampus (inferior temporal horn) and amygdala (superior temporal horn). Our results were based on segmentation of the lateral ventricles and third ventricle, which is amenable to robust automatic segmentation due to the sharp contrast between the signal intensity of CSF and surrounding tissue.

The thalamus, a gray matter structure bordering the third ventricle, is involved in limbic circuitry and mediates or regulates numerous cognitive functions.^{26,27} It is involved in directing attention and suppressing irrelevant sensory input,²⁸ and contributes to the function of memory.²⁹ Size reduction of the thalamus following neurodegeneration has been linked to cognitive performance in Huntington's disease,³⁰ multiple sclerosis³¹ and Alzheimer's disease³². Using automatic segmentation of the thalamus on three-dimensional T1-weighted MR images, De Jong et al. found thalamic volume significantly reduced in patients diagnosed with probable AD.³³ Braak et al. found that extracellular amyloid deposits and neurofibrillary tangles occur in the limbic nuclei of the thalamus.³⁴ As a secondary pathological pathway, subcortical small lesions in the thalamus may disrupt frontal-subcortical circuits, resulting in cognitive impairment of vascular origin superimposed on AD pathology.³⁵ In the current study, persons with subjective memory complaints were found to have a different ventricular shape of the thalamus, suggesting that thalamic atrophy may play a role in the development of subjective memory complaints. The difference in percentage of displaced nodes before versus after FDR correction may be explained by the different p-values employed ($P < 0.01$ versus $P < 0.2$).

The corona radiata, a fibre bundle related to motor function, has been associated with information processing speed.³⁶ Few publications describe a direct relationship between damage to the corona radiata and cognitive performance. Subtle cognitive impairment and emotional disturbances were found in patients with a single lacunar infarct in the corona radiata.³⁷ To our knowledge, changes in the corona radiata have not been described in persons with subjective memory complaints. In the current study, there were no nodes with significant displacement in the ventricular surface of the corona radiata in the uncorrected analysis ($P < 0.01$), and a single node with significant displacement in the ventricular surface of the left corona radiata after FDR correction ($P < 0.2$). This remarkable finding indicates that, in addition to a role in motor function, the corona radiata may also be involved in cognitive function.

The corpus callosum is the largest white matter structure in the brain that connects homologous cortical areas of the two cerebral hemispheres and plays a critical role in

transfer of sensory, cognitive and motor information.³⁸ Callosal atrophy was found to be associated with impaired global cognitive function in a mixed elderly population.³⁹ Wang et al found a significant reduction in corpus callosum volume in persons with subjective memory complaints, compared to controls.⁶ The observed changes of the corpus callosum probably reflect atrophy in the cerebral hemispheres through Wallerian degeneration. Our uncorrected results tentatively concur with the body of evidence that reduction in the volume of the corpus callosum may be associated with subjective memory complaints.

The hippocampus is a small inferior medial temporal lobe structure of a complex shape, which forms part of the limbic system⁴⁰ and plays a central role in memory function.^{41,42} The hippocampus is the site of the earliest neurofibrillary pathology in AD.⁴² Our uncorrected results showed shape differences in the ventricular surface adjacent to the hippocampus in persons with subjective memory complaints. Whether the brain changes in memory complainers are caused by neurofibrillary tangles and amyloid deposits as seen in AD, or ischemic changes is not known. Memory complaints have been associated with AD pathology on post-mortem examination, including both amyloid plaques and neurofibrillary tangles, suggesting that memory complaints in older persons may indicate self-awareness of a degenerative pathologic process.⁵ These early changes may be too subtle for detection by neuropsychological assessments.

The amygdala is a complex structure in the medial temporal lobe consisting of several nuclei.⁴³ It is located superior to the hippocampus, near the superior medial temporal horn. Numerous studies described significant atrophy of the amygdala in AD patients compared to normal controls.^{32,43-45} Whitwell et al. found gray matter loss in the amygdala approximately three years before progression from MCI to AD,⁴⁶ confirming the proposed pathological staging scheme in AD by Braak and Braak.⁴⁷ Striepens et al. reported reduced volumes of the right amygdala in subjective memory impairment.⁴⁸ Our uncorrected results are in accordance with this. However, contrary to previous studies, we did not find significant shape differences in the ventricular surface of the superior medial temporal horn after correction.

Both uncorrected and corrected results showed asymmetric displacement of nodes on the ventricular surface. Asymmetry of hippocampal and amygdalar atrophy has been described in MCI, frontotemporal lobar degeneration (FTLD) and AD.^{8,49-51} In these studies, the structures in the left hemisphere were found to be smaller than in the right hemisphere. Dickerson et al. reported smaller left medial temporal lobe volumes compared to right medial temporal lobe volumes in non-demented patients and in patients with very mild AD.⁵⁰ Barnes et al. compared patterns of hippocampal and

amygdalar atrophy between controls, persons with FTLD and persons with AD and consistently found hippocampal and amygdalar volumes to be smaller on the left side than on the right side, with asymmetry most pronounced in FTLD.⁴⁹ Shi et al. conducted a meta-analysis and found that average volume reduction was stronger in the left hippocampus in both MCI and AD.⁵¹ Van der Flier et al. segmented the hippocampus in persons with subjective memory complaints and observed smaller left hippocampal volumes in patients with subjective memory complaints.⁸ Concurring with earlier reports on left to right asymmetry in cognitive impairment, we found that average displacement of the ventricular shape adjacent to the thalamus was larger on the left side than on the right side using local shape difference analysis. The causes for the observed left versus right asymmetry may be congenital in origin, or as a result of neurodegenerative processes that result in atrophy.

The strengths of the present study include the clear classification of persons into two separate groups through an extensive neuropsychological test battery, as well as the use of a validated automated set-up of our local shape difference analysis method. The study is limited by the indirect assessment of atrophy in periventricular structures through shape differences of the bordering ventricular surface. Nevertheless, manual delineation of the periventricular structures for direct segmentation is limited by an inherent lack of macroscopic contrast of some periventricular structures, as well as an age-related decline of contrast.

In conclusion, the present study demonstrates that the thalamus and the corona radiata may be involved in the pathological changes leading to subjective memory complaints. Uncorrected results show tentative evidence of a role for the corpus callosum, hippocampus and amygdala. The results are promising, but should be interpreted with care.

References

1. Van Oijen M, de Jong FJ, Hofman A, Koudstaal PJ, Breteler MM. Subjective memory complaints, education, and risk of Alzheimer's disease. *Alzheimer's & Dementia* 2007;3:92-97.
2. Gallassi R, Oppi F, Poda R, et al. Are subjective cognitive complaints a risk factor for dementia? *Neurological Sciences* 2010;31:327-336.
3. Mitchell AJ. Is it time to separate subjective cognitive complaints from the diagnosis of mild cognitive impairment? *Age and Ageing* 2008;37:497-499.
4. Glodzik-Sobanska L, Reisberg B, De SS, et al. Subjective memory complaints: presence, severity and future outcome in normal older subjects. *Dementia and Geriatric Cognitive Disorders* 2007;24:177-184.
5. Barnes LL, Schneider JA, Boyle PA, Bienias JL, Bennett DA. Memory complaints are related to Alzheimer disease pathology in older persons. *Neurology* 2006;67:1581-1585.
6. Wang PJ, Saykin AJ, Flashman LA, et al. Regionally specific atrophy of the corpus callosum in AD, MCI and cognitive complaints. *Neurobiology of Aging* 2006;27:1613-1617.
7. Stewart R, Dufouil C, Godin O, et al. Neuroimaging correlates of subjective memory deficits in a community population. *Neurology* 2008;70:1601-1607.
8. Van der Flier WM, van Buchem MA, Weverling-Rijnsburger AW, et al. Memory complaints in patients with normal cognition are associated with smaller hippocampal volumes. *Journal of Neurology* 2004;251:671-675.
9. Van Norden AG, Fick WF, de Laat KF, et al. Subjective cognitive failures and hippocampal volume in elderly with white matter lesions. *Neurology* 2008;71:1152-1159.
10. Ferrarini L, Olofsen H, Palm WM, van Buchem MA, Reiber JH, Admiraal-Behloul F. GAMEs: growing and adaptive meshes for fully automatic shape modeling and analysis. *Medical Image Analysis* 2007;11:302-314.
11. Ferrarini L, Palm WM, Olofsen H, van Buchem MA, Reiber JH, Admiraal-Behloul F. Shape differences of the brain ventricles in Alzheimer's disease. *NeuroImage* 2006;32:1060-1069.
12. Derix MM, Hofstede AB, Teunisse S, et al. [CAMDEX-N: the Dutch version of the Cambridge Examination for Mental Disorders of the Elderly with automatic data processing]. *Tijdschrift voor Gerontologie en Geriatrie* 1991;22:143-150.
13. Roth M, Tym E, Mountjoy CQ, et al. CAMDEX. A standardised instrument for the diagnosis of mental disorder in the elderly with special reference to the early detection of dementia. *British Journal of Psychiatry* 1986;149:698-709.
14. Folstein MF, Folstein SE, McHugh PR. "Mini-mental state". A practical method for grading the cognitive state of patients for the clinician. *Journal of Psychiatric Research* 1975;12:189-198.
15. Wechsler DA. A standardized memory scale for clinical use. *Journal of Psychology* 1945;19:87-95.
16. Rosen WG, Mohs RC, Davis KL. A new rating scale for Alzheimer's disease. *American Journal of Psychiatry* 1984;141:1356-1364.
17. Kaplan E, Goodglass H, Weintraub S. Boston naming test, 2nd edition. Austin: Pro-ed; 2001. 60 p.
18. Benton AL, Hamsler K. Multilingual aphasia examination, 2nd edition. Iowa City: AJA Associates; 1983. 30 p.
19. Reitan RM. Validity of the Trail Making Test as an indicator of organic brain damage. *Perceptual and Motor Skills* 1958;8:271-276.
20. Wechsler DA. Wechsler Adult Intelligence Scale—Revised. New York: Psychological Corporation; 1981. 156 p.
21. Admiraal-Behloul F, van den Heuvel DM, Olofsen H, et al. Fully automatic segmentation of white matter hyperintensities in MR images of the elderly. *NeuroImage* 2005;28:607-617.
22. Woods RP, Grafton ST, Holmes CJ, Cherry SR, Mazziotta JC. Automated image registration: I. General methods and intrasubject, intramodality validation. *Journal of Computer Assisted Tomography* 1998;22:139-152.

23. Ferrarini L, Palm WM, Olofsen H, et al. Ventricular shape biomarkers for Alzheimer's disease in clinical MR images. *Magnetic Resonance in Medicine* 2008;59:260-267.
24. Kohonen T. The self-organizing map. *Proceedings of the IEEE* 1990;78:1464-1480.
25. Weir J, Abrahams PH, Spratt JD, et al. *Imaging Atlas of Human Anatomy*, 3rd edition. Edinburgh: Mosby; 2003. 224 p.
26. Aggleton JP, Brown MW. Episodic memory, amnesia, and the hippocampal-anterior thalamic axis. *Behavioral and Brain Sciences* 1999;22:425-444.
27. Stein T, Moritz C, Quigley M, Cordes D, Haughton V, Meyerand E. Functional connectivity in the thalamus and hippocampus studied with functional MR imaging. *AJNR American Journal of Neuroradiology* 2000;21:1397-1401.
28. Newman J. Thalamic contributions to attention and consciousness. *Consciousness and Cognition* 1995;4:172-193.
29. Van der Werf YD, Witter MP, Uylings HB, Jolles J. Neuropsychology of infarctions in the thalamus: a review. *Neuropsychologia* 2000;38:613-627.
30. Kassubek J, Juengling FD, Ecker D, Landwehrmeyer GB. Thalamic atrophy in Huntington's disease covaries with cognitive performance: a morphometric MRI analysis. *Cerebral Cortex* 2005;15:846-853.
31. Houtchens MK, Benedict RH, Killiany R, et al. Thalamic atrophy and cognition in multiple sclerosis. *Neurology* 2007;69:1213-1223.
32. Callen DJ, Black SE, Gao F, Caldwell CB, Szalai JP. Beyond the hippocampus: MRI volumetry confirms widespread limbic atrophy in AD. *Neurology* 2001;57:1669-1674.
33. De Jong LW, van der Hiele K, Veer IM, et al. Strongly reduced volumes of putamen and thalamus in Alzheimer's disease: an MRI study. *Brain* 2008;131:3277-3285.
34. Braak H, Braak E. Alzheimer's disease affects limbic nuclei of the thalamus. *Acta Neuropathologica* 1991;81:261-268.
35. Mori E. Impact of subcortical ischemic lesions on behavior and cognition. *Annals of the New York Academy of Sciences* 2002;977:141-148.
36. Sasson E, Doniger GM, Pasternak O, Tarrasch R, Assaf Y. Structural correlates of cognitive domains in normal aging with diffusion tensor imaging. *Brain Structure and Function* 2012;217:503-515.
37. Van Zandvoort MJ, Kappelle LJ, Algra A, de Haan EH. Decreased capacity for mental effort after single supratentorial lacunar infarct may affect performance in everyday life. *Journal of Neurology, Neurosurgery & Psychiatry* 1998;65:697-702.
38. Perez MA, Cohen LG. Interhemispheric inhibition between primary motor cortices: what have we learned? *Journal of Physiology* 2008;
39. Ryberg C, Rostrup E, Stegmann MB, et al. Clinical significance of corpus callosum atrophy in a mixed elderly population. *Neurobiology of Aging* 2007;28:955-963.
40. Tarroun A, Bonnefoy M, Bouffard-Vercelli J, Gedeon C, Vallee B, Cotton F. Could linear MRI measurements of hippocampus differentiate normal brain aging in elderly persons from Alzheimer disease? *Surgical and Radiologic Anatomy* 2007;29:77-81.
41. Arriagada PV, Growdon JH, Hedley-Whyte ET, Hyman BT. Neurofibrillary tangles but not senile plaques parallel duration and severity of Alzheimer's disease. *Neurology* 1992;42:631-639.
42. Braak H, Braak E. Neuropathological staging of Alzheimer-related changes. *Acta Neuropathologica* 1991;82:239-259.
43. Hensel A, Wolf H, Dieterlen T, Riedel-Heller S, Arendt T, Gertz HJ. Morphometry of the amygdala in patients with questionable dementia and mild dementia. *Journal of the Neurological Sciences* 2005;238:71-74.
44. Basso M, Yang J, Warren L, et al. Volumetry of amygdala and hippocampus and memory performance in Alzheimer's disease. *Psychiatry Research* 2006;146:251-261.
45. Cuenod CA, Denys A, Michot JL, et al. Amygdala atrophy in Alzheimer's disease. An in vivo magnetic resonance imaging study. *Archives of Neurology* 1993;50:941-945.

46. Whitwell JL, Przybelski SA, Weigand SD, et al. 3D maps from multiple MRI illustrate changing atrophy patterns as subjects progress from mild cognitive impairment to Alzheimer's disease. *Brain* 2007;130:1777-1786.
47. Braak H, Braak E. Evolution of the neuropathology of Alzheimer's disease. *Acta Neurologica Scandinavica Supplement* 1996;165:3-12.
48. Striepens N, Scheef L, Wind A, et al. Volume loss of the medial temporal lobe structures in subjective memory impairment. *Dementia and Geriatric Cognitive Disorders* 2010;29:75-81.
49. Barnes J, Whitwell JL, Frost C, Josephs KA, Rossor M, Fox NC. Measurements of the amygdala and hippocampus in pathologically confirmed Alzheimer disease and frontotemporal lobar degeneration. *Archives of Neurology* 2006;63:1434-1439.
50. Dickerson BC, Goncharova I, Sullivan MP, et al. MRI-derived entorhinal and hippocampal atrophy in incipient and very mild Alzheimer's disease. *Neurobiology of Aging* 2001;22:747-754.
51. Shi F, Liu B, Zhou Y, Yu C, Jiang T. Hippocampal volume and asymmetry in mild cognitive impairment and Alzheimer's disease: Meta-analyses of MRI studies. *Hippocampus* 2009;19:1055-1064.

4

Intracranial compartment volumes in normal pressure hydrocephalus: volumetric assessment versus outcome

American Journal of Neuroradiology.
2006;27(1):76-9

W.M. Palm
R. Walchenbach
B. Bruinsma
F. Admiraal-Behloul
H.A.M. Middelkoop
L.J. Launer
J. van der Grond
M.A. van Buchem

Abstract

Although enlargement of the cerebral ventricles plays a central role in the diagnosis of Normal Pressure Hydrocephalus (NPH), there are no reports on the use of volumetric assessment to distinguish between patients who respond to ventriculoperitoneal shunting and those who do not. The purpose of the present study is to explore the association between pre-operative intracranial compartment volumes and postoperative improvement.

Twenty-six patients (17 men, mean age 75 years [range: 54 – 87 years]) with a clinical or radiological suspicion of NPH were included in the study. Gait, cognition and bladder function were evaluated by clinical rating. MR imaging of the brain was acquired at 0.5T and 1.5T. Total intracranial volume, ventricular volume, brain volume and pericerebral CSF volume were determined by volumetric assessment. Four imaging variables were determined: ventricular volume ratio, brain volume ratio, pericerebral CSF volume ratio and the ratio between ventricular volume and pericerebral CSF volume. All patients underwent ventriculoperitoneal shunting.

Clinical follow-up was assessed one year after shunting. No difference in the mean ventricular volume ratio, the mean brain volume ratio, the mean pericerebral CSF volume ratio and the mean ratio between ventricular and pericerebral CSF volume was found between subjects who improved on gait or cognition or bladder function and those who did not.

Volumetric assessment has no predictive value in differentiating between NPH patients who respond to ventriculoperitoneal shunting and those who do not.

Introduction

Forty years ago, Adams et al. described a syndrome that combined a clinical triad of gait impairment, cognitive impairment and urinary incontinence with normal cerebrospinal fluid pressure.¹ The clinical triad together with enlargement of the cerebral ventricles on Computed Tomography (CT) or Magnetic Resonance (MR) imaging is suggestive for the Normal Pressure Hydrocephalus (NPH) syndrome.² The uniqueness of this syndrome lies in the partial reversibility of the symptoms after the insertion of a ventricular shunt.¹ Despite high morbidity rates,³ and lack of evidence indicating that shunt placement is effective in the management of NPH,⁴ shunting remains the standard treatment.⁵ Many diagnostic procedures have been described that may increase the probability of selecting the appropriate candidates for shunting. Factors that predict a good surgical outcome are substantial improvement after one or several lumbar cerebrospinal fluid (CSF) taps,⁶⁻⁷ substantial improvement after continuous external lumbar CSF drainage,⁸⁻¹⁰ occurrence of B-waves more than 50% of the recording time during continuous intracranial pressure monitoring,¹¹⁻¹⁵ resistance to CSF outflow of 18 mm Hg/ml per minute or higher during continuous lumbar CSF infusion test,^{12,16} or the observation on MR imaging of increased CSF flow through the aqueduct.¹⁷⁻¹⁸

Volumetric assessment of intracranial compartments has been used to distinguish NPH patients from healthy subjects and to set the syndrome apart from obstructive hydrocephalus, brain atrophy, cerebrovascular disease, vascular dementia or Alzheimer's disease.¹⁹⁻²⁵ Given the important role of enlargement of the cerebral ventricles in the diagnosis of NPH, a quantitative approach of ventricle size could be useful for the selection of patients for ventriculoperitoneal shunting. There are no previous reports on the use of volumetric assessment to distinguish between patients who respond to ventriculoperitoneal shunting and those who do not.

In the present study, volumetric measurements were performed in patients with clinical NPH to study the association of preoperative intracranial compartment volumes with postoperative outcome. The preoperative ventricular volume, brain volume, pericerebral CSF volume, and the ratio between ventricular volume and pericerebral CSF volume were quantified and correlated with postoperative improvement in gait impairment, cognitive impairment and urinary incontinence.

Methods

Patients

All patients with presumed NPH referred to our Department of Neurosurgery between 1995 and 2001 were invited to participate. The diagnosis of NPH was made by independent neurologists from our hospital's neurological department or neurological departments from surrounding regional hospitals. When the neurologist diagnosed NPH, both conservative and operative management possibilities were discussed with the patient. If the patient chose a surgical approach he was referred to the neurosurgeon. Of the 28 patients that fulfilled the criteria of presumed NPH, 26 consented to participate in our study (17 males, mean age 75 years, median age 77 years, range 54 to 87 years). Inclusion criteria were the following: wide based gait imbalance or small stepped shuffling gait, and dilated lateral and third ventricles in combination with a frontal horn index (the ratio between the maximal width of the frontal horns and the width of the whole brain at the same level)²⁶ of 0.40 or higher.²⁷ Neither cognitive impairment nor bladder dysfunction was required for inclusion. Patients presenting with dementia of the Alzheimer's type were excluded. Informed consent was obtained for all patients.

Clinical examinations

Gait and bladder function were evaluated by one of us, an experienced neurosurgeon (R.W.). Gait impairment was rated on a five point scale: (0) normal, (1) slight gait imbalance, (2) marked gait imbalance but not requiring aid, (3) walking not possible without a cane or the help of one person, (4) gait severely impaired, only possible with the aid of one person on each side, (5) total incapacity for standing or walking, even with help.²⁷ Bladder function was registered as (0) normal, (1) increased bladder urgency, and (2) urinary incontinence. Cognitive function was assessed with an extensive neuropsychological test battery by one of us, an experienced clinical neuropsychologist (H.M.).

MR image acquisition and processing

MR brain imaging was performed in all patients prior to ventriculoperitoneal shunting. Dual spin-echo (proton density and T2 weighted) images were acquired at field strengths of 0.5T (n=7) or 1.5T (n=19) (Philips Medical Systems, Best, The Netherlands) with 2500 ms repetition time, 27/120 ms echo time, a 256 x 256 matrix and 6 mm slice thickness with 0.6 mm interslice gap, covering the whole brain. Locally developed semi-automated segmentation software (SNIPER, Software for Neuro-Image Processing in Experimental Research) that combines knowledge-based fuzzy clustering and region-growing techniques was used to process the images.²⁸ The outer contour of the

subarachnoid space was manually delineated on each slice by one observer (W.P.), which was followed by an automated segmentation procedure that assigned brain tissue and CSF within this region (Figure 5.1). The volumetric assessment was repeated for five out of 26 subjects (19%) to analyze the intra-rater reliability. The intra-class correlation coefficient was larger than 0.99, indicating high intra-rater reliability. We determined total intracranial volume (TICV, comprising brain parenchyma and CSF), total brain volume (TBV), ventricular CSF volume (VV, comprising lateral, third and fourth ventricles) and extraventricular CSF volume (EVV, reflecting pericerebral CSF volume). Ventricular volume, brain volume and pericerebral CSF volume were converted into ratios from total intracranial volume to normalize for head size. Ventriculomegaly out of proportion to cortical sulcal enlargement, a neuro-imaging characteristic of NPH,^{18;29-31} was quantified by dividing ventricular volume by pericerebral CSF volume. In summary, four imaging variables were obtained: ventricular volume ratio, brain volume ratio, pericerebral CSF volume ratio and a ratio between ventricular and pericerebral CSF volume.

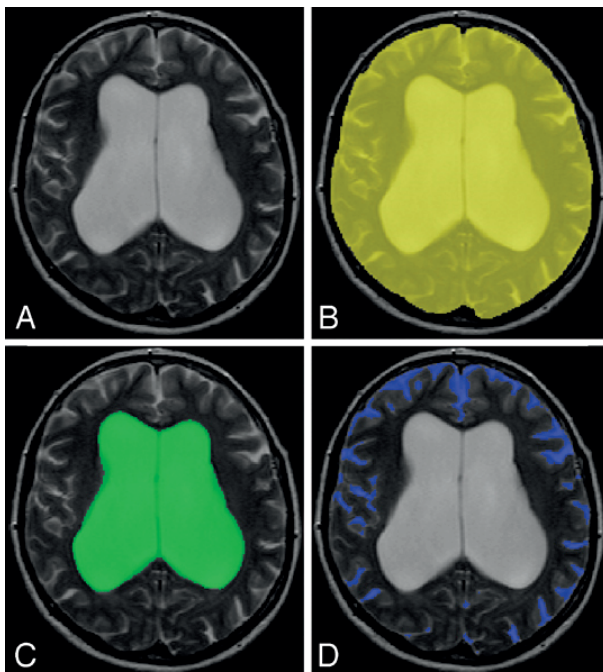


Figure 5.1

Intracranial semi-automated segmentation was based on axial T2 (A) and proton density weighted images. The outer contour of the subarachnoid space was manually delineated on each slice (B). This was followed by an automated segmentation procedure that assigned brain tissue and CSF within this region. We determined total intracranial volume, ventricular volume (C), brain volume and pericerebral CSF volume (D).

Ventriculoperitoneal shunting

All patients underwent ventriculoperitoneal shunting. The type of shunt was a Codman-Medos non-programmable valve system with an opening pressure of 100 mm H₂O. The patency of the shunt was judged by a neurosurgeon through clinical examination at 2, 6, and 12 months after ventriculoperitoneal shunting. In patients with lack of amelioration or clinical deterioration in combination with lack of decrease of the ventricular volume on CT or MR imaging, a surgical drain revision was carried out. The subjects remained shunted during the entire follow-up period of one year after shunt placement.

Statistical methods

The mean ventricular volume ratio, the mean brain volume ratio, the mean pericerebral CSF volume ratio and the mean ratio between ventricular and pericerebral CSF volume were compared between the patients that improved after shunting and those who did not. Improvement of gait, improvement of cognition and improvement of bladder function were determined by clinical rating (R.W. and H.M. respectively).²⁷ Mann-Whitney U tests were applied to assess differences between the four imaging variables and improvement in gait or cognition or bladder function (SPSS, version 11.5; SPSS Inc., Chicago, IL). Adjustments were made for multiple comparisons using the Bonferroni method. The level of statistical significance was set at $p < 0.05$.

Results

All 26 patients had gait impairment, 22 were cognitively impaired and 22 suffered from urinary incontinence. Clinical follow-up for the assessment of treatment effect took place one year after shunting. Three had died in the follow-up period and were excluded from our analysis. After shunting, 19 out of 23 remaining patients (83%) with preoperative gait impairment showed an improved walking pattern. Nine out of 19 remaining patients (47%) with preoperative cognitive impairment showed improved cognition after shunting. Nine out of 20 remaining patients (45%) with preoperative bladder dysfunction reported a decrease in urinary urgency or urinary incontinence after shunting.

Baseline values of total intracranial volume, ventricular volume, brain volume and extraventricular volume for all subjects are presented in Table 5.1. The mean and standard deviation of the four imaging variables are presented in Table 5.2, classified into improvement in each of the symptoms from the NPH clinical triad.

Table 5.1 Baseline MR imaging values

	Mean (in cc)	SD
Total intracranial volume	1533.98	133.32
Ventricular volume	156.25	46.20
Brain volume	1176.50	105.07
Pericerebral CSF volume	201.23	37.89

MR: Magnetic resonance, SD: Standard deviation, CSF: Cerebrospinal fluid

Table 5.2 Mean and standard deviation of the four imaging variables, classified into improvement per symptom.

Gait	Not Improved n=4	Improved n=19
Ventricular volume ratio	0.11 (\pm 0.01)	0.11 (\pm 0.03)
Brain volume ratio	0.76 (\pm 0.02)	0.77 (\pm 0.03)
Pericerebral CSF volume ratio	0.13 (\pm 0.02)	0.13 (\pm 0.02)
Ratio between ventricular and pericerebral CSF volume	0.85 (\pm 0.14)	0.85 (\pm 0.28)
Cognition	Not Improved n=10	Improved n=9
Ventricular volume ratio	0.10 (\pm 0.03)	0.11 (\pm 0.02)
Brain volume ratio	0.77 (\pm 0.03)	0.76 (\pm 0.02)
Pericerebral CSF volume ratio	0.13 (\pm 0.02)	0.12 (\pm 0.02)
Ratio between ventricular and pericerebral CSF volume	0.81 (\pm 0.28)	0.96 (\pm 0.22)
Bladder function	Not Improved n=4	Improved n=19
Ventricular volume ratio	0.11 (\pm 0.03)	0.10 (\pm 0.02)
Brain volume ratio	0.76 (\pm 0.03)	0.78 (\pm 0.02)
Pericerebral CSF volume ratio	0.13 (\pm 0.02)	0.12 (\pm 0.01)
Ratio between ventricular and pericerebral CSF volume	0.84 (\pm 0.29)	0.91 (\pm 0.25)

Ventricular volume, brain volume and pericerebral CSF volume were converted into ratios from total intracranial volume to normalize for head size. CSF: Cerebrospinal Fluid

The mean of the four imaging variables - ventricular volume ratio, brain volume ratio, pericerebral CSF volume ratio and ratio between ventricular volume and pericerebral CSF volume - did not differ significantly between patients who experienced improvement in gait after shunting and those who did not. No significant differences were found in the mean of the four imaging variables between patients who improved in cognition and those who maintained the same level of cognitive impairment. There

were also no significant differences in the mean of the four imaging variables between patients who did not report an improvement in bladder function and those who did experience less urinary urgency or urinary incontinence after shunting.

Discussion

Our most important finding is that the mean ventricular volume ratio, the mean brain volume ratio, the mean pericerebral CSF volume ratio nor the mean ratio between ventricular and pericerebral CSF volume were different between NPH patients who improved on gait or cognition or bladder function after ventriculoperitoneal shunting and those who did not.

Our results suggest that volumetric assessment of intracranial compartments has no predictive value in differentiating between NPH patients who will respond favorably to ventriculoperitoneal shunting and those who will not. Volumetric assessment has previously been employed to set NPH apart from other conditions and healthy elderly.²²⁻²³ The technique has not been used to compare intracranial compartment volumes between NPH patients who improved after ventriculoperitoneal shunting and those who did not. In one study MR brain images were used to study the pre-operative neuro-imaging characteristics of NPH in relation to clinical outcome after ventriculoperitoneal shunting.³² In this study, CT and MR brain images were independently evaluated in a qualitative way by a neuroradiologist, showing an association between pre-operative cortical sulci size and post-operative improvement in gait, cognition and bladder function, whereas ventricular volume was unrelated to post-operative outcome. The finding of an association between pre-operative cortical sulci size or pericerebral CSF volume and outcome was not reproduced in our study.

A potential limitation of our study is that all the included subjects were patients eligible for shunting. This resulted in the lack of a control group and a moderate spread of values. Still, it should be realized that our population represents a consecutive clinical group eligible for shunting, which is the group that benefits most from pre-operative risk stratification. In addition, if ventricular volume stays the same after the shunt is placed, and the patient does not get better, then a shunt function study needs to be done to determine if the shunt is indeed functioning in light of the fact that the volume of the ventricles has not changed.

Conclusion

The ventricular volume ratio, brain volume ratio, pericerebral CSF volume ratio nor the ratio between ventricular and pericerebral CSF volume were different between NPH patients who improved on gait or cognition or bladder function and those who did not. Volumetric assessment of intracranial compartments has no predictive value in differentiating between NPH patients who will respond favorably to ventriculoperitoneal shunting and those who will not.

Reference List

1. Adams RD, Fisher CM, Hakim S, Ojemann RG, Sweet WH. Symptomatic occult hydrocephalus with "normal" cerebrospinal-fluid pressure. A treatable syndrome. *New England Journal of Medicine* 1965;273:117-126
2. Vanneste JA. Diagnosis and management of normal-pressure hydrocephalus. *Journal of Neurology* 2000;247:5-14
3. Hebb AO, Cusimano MD. Idiopathic normal pressure hydrocephalus: a systematic review of diagnosis and outcome. *Neurosurgery* 2001;49:1166-1184
4. Esmonde T, Cooke S. Shunting for normal pressure hydrocephalus (NPH). *Cochrane Database Syst Rev* 2002;CD003157
5. Bret P, Guyotat J, Chazal J. Is normal pressure hydrocephalus a valid concept in 2002? A reappraisal in five questions and proposal for a new designation of the syndrome as "chronic hydrocephalus". *Journal of Neurology, Neurosurgery and Psychiatry* 2002;73:9-12
6. Sand T, Bovim G, Grimse R, Myhr G, Helde G, Cappelen J. Idiopathic normal pressure hydrocephalus: the CSF tap-test may predict the clinical response to shunting. *Acta Neurologica Scandinavica* 1994;89:311-316
7. Wikkelso C, Andersson H, Blomstrand C, Lindqvist G, Svendsen P. Normal pressure hydrocephalus. Predictive value of the cerebrospinal fluid tap-test. *Acta Neurologica Scandinavica* 1986;73:566-573
8. Chen IH, Huang CI, Liu HC, Chen KK. Effectiveness of shunting in patients with normal pressure hydrocephalus predicted by temporary, controlled-resistance, continuous lumbar drainage: a pilot study. *Journal of Neurology, Neurosurgery and Psychiatry* 1994;57:1430-1432
9. Di Lauro L, Mearini M, Bollati A. The predictive value of 5 days CSF diversion for shunting in normal pressure hydrocephalus. *Journal of Neurology, Neurosurgery and Psychiatry* 1986;49:842-843
10. Haan J, Thomeer RT. Predictive value of temporary external lumbar drainage in normal pressure hydrocephalus. *Neurosurgery* 1988;22:388-391
11. Borgesen SE, Gjerris F. The predictive value of conductance to outflow of CSF in normal pressure hydrocephalus. *Brain* 1982;105:65-86
12. Bret P, Chazal J, Janny P, et al. [Chronic hydrocephalus in adults]. *Neurochirurgie* 1990;36 Suppl 1:1-159
13. Crockard HA, Hanlon K, Duda EE, Mullan JF. Hydrocephalus as a cause of dementia: evaluation by computerised tomography and intracranial pressure monitoring. *Journal of Neurology, Neurosurgery and Psychiatry* 1977;40:736-740
14. Pickard JD, Teasdale G, Matheson M, et al. Intraventricular pressure waves - the best predictive test for shunting in normal pressure hydrocephalus. In: Shulman K, Marmarou A, Miller J D, et al, eds. *Intracranial pressure IV*. Berlin: Springer; 1980;498-500
15. Symon L, Dorsch NW. Use of long-term intracranial pressure measurement to assess hydrocephalic patients prior to shunt surgery. *Journal of Neurosurgery* 1975;42:258-273
16. Boon AJ, Tans JT, Delwel EJ, et al. Dutch normal-pressure hydrocephalus study: prediction of outcome after shunting by resistance to outflow of cerebrospinal fluid. *Journal of Neurosurgery* 1997;87:687-693
17. Bradley WG, Jr., Whittemore AR, Kortman KE, et al. Marked cerebrospinal fluid void: indicator of successful shunt in patients with suspected normal-pressure hydrocephalus. *Radiology* 1991;178:459-466
18. Bradley WG, Jr., Scalzo D, Queralt J, Nitz WN, Atkinson DJ, Wong P. Normal-pressure hydrocephalus: evaluation with cerebrospinal fluid flow measurements at MR imaging. *Radiology* 1996;198:523-529
19. Condon B, Patterson J, Wyper D, et al. Use of magnetic resonance imaging to measure intracranial cerebrospinal fluid volume. *Lancet* 1986;1:1355-1357

20. Kitagaki H, Mori E, Ishii K, Yamaji S, Hirono N, Imamura T. CSF spaces in idiopathic normal pressure hydrocephalus: morphology and volumetry. *AJNR American Journal of Neuroradiology* 1998;19:1277-1284
21. Matsumae M, Kikinis R, Morocz I, et al. Intracranial compartment volumes in patients with enlarged ventricles assessed by magnetic resonance-based image processing. *Journal of Neurosurgery* 1996;84:972-981
22. Tsunoda A, Mitsuoka H, Sato K, Kanayama S. A quantitative index of intracranial cerebrospinal fluid distribution in normal pressure hydrocephalus using an MRI-based processing technique. *Neuroradiology* 2000;42:424-429
23. Tsunoda A, Mitsuoka H, Bandai H, Arai H, Sato K, Makita J. Intracranial cerebrospinal fluid distribution and its postoperative changes in normal pressure hydrocephalus. *Acta Neurochirurgica (Wien)* 2001;143:493-499
24. Tsunoda A, Mitsuoka H, Bandai H, Endo T, Arai H, Sato K. Intracranial cerebrospinal fluid measurement studies in suspected idiopathic normal pressure hydrocephalus, secondary normal pressure hydrocephalus, and brain atrophy. *Journal of Neurology, Neurosurgery and Psychiatry* 2002;73:552-555
25. Yoshihara M, Tsunoda A, Sato K, Kanayama S, Calderon A. Differential diagnosis of NPH and brain atrophy assessed by measurement of intracranial and ventricular CSF volume with 3D FASE MRI. *Acta Neurochirurgica Supplement* 1998;71:371-374
26. Gyldensted C. Measurements of the normal ventricular system and hemispheric sulci of 100 adults with computed tomography. *Neuroradiology* 1977;14:183-192
27. Walchenbach R, Geiger E, Thomeer RT, Vanneste JA. The value of temporary external lumbar CSF drainage in predicting the outcome of shunting on normal pressure hydrocephalus. *Journal of Neurology, Neurosurgery and Psychiatry* 2002;72:503-506
28. Van den Boom R, Lesnik Oberstein SA, Spilt A, et al. Cerebral hemodynamics and white matter hyperintensities in CADASIL. *Journal of Cerebral Blood Flow Metabolism* 2003;23:599-604
29. Bradley WG. Normal pressure hydrocephalus: new concepts on etiology and diagnosis. *AJNR American Journal of Neuroradiology* 2000;21:1586-1590
30. Fishman RA, Dillon WP. Normal pressure hydrocephalus: new findings and old questions. *AJNR American Journal of Neuroradiology* 2001;22:1640-1641
31. Jack CR, Jr., Lexa FJ, Trojanowski JQ, Braffman BH, Atlas SW. Normal Aging, Dementia, and Neurodegenerative Disease. In: Atlas SW, ed. *Magnetic Resonance Imaging of the Brain and Spine* 3rd ed. Philadelphia, Pa: Lippincott Williams & Wilkins; 2001;1177-1240
32. Poca MA, Mataro M, Del Mar MM, Arikian F, Junque C, Sahuquillo J. Is the placement of shunts in patients with idiopathic normal-pressure hydrocephalus worth the risk? Results of a study based on continuous monitoring of intracranial pressure. *Journal of Neurosurgery* 2004;100:855-866

5

Ventricular dilatation: association with gait and cognition

Annals of Neurology. 2009;66(4):485-93

W.M. Palm
J.S. Saczynski
J. van der Grond
S. Sigurdsson
O. Kjartansson
P.V. Jonsson
G. Eiriksdottir
V. Gudnason
F. Admiraal-Behloul
L.J. Launer
M.A. van Buchem

Abstract

Normal Pressure Hydrocephalus is characterized by gait impairment, cognitive impairment and urinary incontinence, and is associated with disproportionate ventricular dilation. Here we report the distribution of ventricular volume relative to sulcal CSF volume, and the association of increasing ventricular volume relative to sulcal CSF volume with a cluster of gait impairment, cognitive impairment and urinary incontinence in a stroke-free cohort of elderly persons from the general population.

Data are based on 858 persons (35.4 % men, age range 66-92 years) who participated in the Age, Gene/Environment Susceptibility Study - Reykjavik Study. Gait was evaluated with an assessment of gait speed. Composite scores representing speed of processing, memory and executive function were constructed from a neuropsychological battery. Bladder function was assessed with a questionnaire. MR brain imaging was followed by semi-automated segmentation of intracranial CSF volume. White matter hyperintensity (WMH) volume was assessed with a semi-quantitative scale. For the analysis of ventricular dilation relative to the sulcal spaces, ventricular volume was divided by sulcal CSF volume (VV/SV).

Disproportion between ventricular and sulcal CSF volume, defined as the highest quartile of the VV/SV Z score, was associated with gait impairment (OR 1.9, 95% CI 1.1 – 3.3), and cognitive impairment (OR 1.8, 95% CI 1.1 – 3.0). We did not find an association between the VV/SV Z-score and bladder dysfunction.

The prevalence and severity of gait impairment and cognitive impairment increases with ventricular dilation in persons without stroke from the general population, independent of WMH volume.

Introduction

Cerebral atrophy is a pathologic diagnosis indicating an irreversible loss of brain substance.^{1,2} It appears as progressive dilation of the ventricles and cortical sulci on Magnetic Resonance (MR) imaging.¹ Global cerebral atrophy is often classified into sub-cortical atrophy, reflecting ventricular dilation, and cortical atrophy, reflecting the dilation of cortical sulci.³

Sub-cortical atrophy and cortical atrophy may not be in proportion with each other (Figure 6.1). When the amount of sub-cortical atrophy corresponds with the amount of cortical atrophy, this may be indicative of global cerebral atrophy, as seen with increasing age. However, when a disproportion between ventricular dilation and the dilation of sulcal CSF volume is noted (Figure 6.1), Normal Pressure Hydrocephalus (NPH) may be suggested, when these MRI findings are associated with gait impairment, cognitive and urinary urgency or incontinence.⁴⁻⁷ Suspicion of NPH is increased when gait imbalance predominates and when cognitive deficit is only slight, moderate, or even absent.⁸ When dementia is the most severe symptom, the probability of NPH is very low.^{9,10} Bladder dysfunction occurs only at later stages of NPH and is present in approximately 55 percent of patients with NPH.^{9,10} Thus, based on previous work, the complete triad can be observed in nearly half of NPH patients.⁹



Figure 6.1

In this example, the volume of the ventricles is out of proportion to the volume of the sulcal spaces.

The different clinical components of the NPH triad are each highly prevalent in older persons. Gait disorders affect 20% to 50% of elderly persons.^{11,12} Prevalence studies of dementing illnesses suggest an overall prevalence rate of about 6% to 8% among individuals older than 65 years and a prevalence rate of over 30% among individuals

older than 85 years.^{13,14} The prevalence of at least some degree of bladder dysfunction is estimated at 11% to 31% of men aged 60 years and older¹⁵ and at 30% to 50% of elderly women.¹⁶ It is not known to what extent gait impairment, cognitive impairment and bladder dysfunction cluster together in the general population of older adults. Furthermore, patients with white matter hyperintensities (WMH) or subcortical arteriosclerotic encephalopathy often present with an enlarged ventricular system and symptoms and signs similar to those seen in NPH.¹⁷⁻¹⁹

Here we report on the prevalence of clusters of gait impairment, cognitive impairment and bladder dysfunction and their association with ventricular dilation, independent of WMH volume.

Methods

Persons participating in this study were a sample of the Age, Gene/Environment Susceptibility (AGES) – Reykjavik Study; a population-based study initiated to examine the contribution of genetic susceptibility and gene/environment interaction to conditions common in old age. The AGES – Reykjavik Study is an extension of the Reykjavik Study (RS) (1967-1994), a prospective study of cardiovascular disease based on a cohort of men and women born 1907-1935 and living in Reykjavik at the time of baseline measure in 1967.^{20,21} All participants in the AGES - Reykjavik Study underwent extensive evaluation, including MRI of the brain, neuropsychological testing, physical performance, a standard clinical evaluation, and an in-person questionnaire. This report is based on those participants examined from September 2002 until March 2004 (n = 2,300). The protocol was approved by the Icelandic National Bioethics Committee (VSN 00-063), the Icelandic Data Protection Authority, and by the Institutional Review Board of the US National Institutes of Health.²²

Measurement of gait

Gait was evaluated as the time in seconds needed to walk 6 meters. There were two measurements at usual pace and separately two at quick pace.²³⁻²⁵ The two measurements for usual pace and quick pace were averaged separately for one estimate of normal gait and one for fast gait. Since there are no standardized cut-points for impaired gait speed in the 6-meter walk test, the upper quartile in either normal or fast gait was defined as gait impairment, similar to previous studies.^{26,27}

Measurement of cognitive function

Composite scores of executive function, memory and speed of processing were constructed from a battery of neuropsychological tests. The fit of these theoretical composites has been described in a previous publication.²⁸ The executive function composite consisted of: the Digits Backward,²⁹ the CANTAB spatial working memory task,³⁰ and the Stroop Test Part III³¹. The memory composite consisted of: California Verbal Learning Test immediate and delayed recall.³² The speed of processing composite consisted of: the Digit Symbol Substitution Test,²⁹ Figure Comparison,³³ and the Stroop Test Parts I and II.³¹ All tests were normally distributed, thus composite measures were computed by averaging z-scores. A diagnosis of dementia - established in a multidisciplinary consensus meeting - was used to control for the possibility that cognitive impairment was partly due to comorbidities, such as Alzheimer's Disease.

Measurement of bladder function

Bladder function was assessed with a standard questionnaire. Dysfunction, when present, was characterized into (1) urinary incontinence associated with an activity like coughing, lifting, standing up or exercise (2) urge incontinence where the subject cannot get to the toilet fast enough and (3) urinary incontinence unrelated to coughing, sneezing, lifting or urge. Normal Pressure Hydrocephalus (NPH) type bladder dysfunction was defined as positive answers to questions 2 or 3, corresponding with descriptions in literature.^{4,10,34}

MR image acquisition and post-processing

The current analyses required dual fast spin-echo (proton density (PD) and T2-weighted) and Fluid-Attenuated Inversion Recovery (FLAIR) images, which were acquired at a field strength of 1.5T (GE Medical Systems, Milwaukee, Wisconsin). The PD- and T2-weighted scans were performed with a field of view of 220 mm, a 256 x 256 matrix size, section thickness of 3.0 mm and no slice gap. The FLAIR scans were performed with a field of view of 220 mm, a 256 x 256 matrix size, section thickness of 3.0 mm and no slice gap.

Cerebral infarcts were defined as lesions 4 mm or larger in the maximum diameter over a vascular distribution with typical MRI characteristics (e.g. a signal intensity that was isointense to that of cerebrospinal fluid), and were distinguished from WMHs.

Cerebellar infarcts had no size criteria since lesions in this area can be very small. A neuroradiologist first examined the images for presence of cortical, subcortical, and cerebellar infarcts. Then, radiographers characterized the infarcts in more detail. WMH volume was assessed with a semi-quantitative scale with known reliability and validity.³⁵

To analyze the scans we used previously described automated segmentation software (SNIPER, Software for Neuro-Image Processing in Experimental Research) that combines knowledge-based fuzzy clustering and region-growing techniques.³⁵ The dual fast spin-echo and FLAIR images were co-registered using FMRIB's Linear Imaging Regression Tool (FLIRT)³⁶ prior to processing by SNIPER. Brain extraction was followed by an automated segmentation procedure that assigned CSF within the cranium. CSF belonging to the lateral and third ventricles was manually labeled as ventricular volume by an experienced reader (W.M.P.). The volumetric assessment was repeated for 43 out of 834 persons (5%) to analyze the intra-rater reliability in our sample. The assessment yielded an intra-class correlation coefficient greater than 0.99, indicating high intra-rater reliability. The program estimated ventricular volume (VV), sulcal CSF volume (SV), total brain volume (TBV) and total intracranial volume (TICV). To express ventricular dilation relative to the volume of the sulcal spaces, ventricular volume was divided by sulcal CSF volume (VV/SV) (Figure 6.2). TBV/TICV was used as a measure of corrected brain volume.

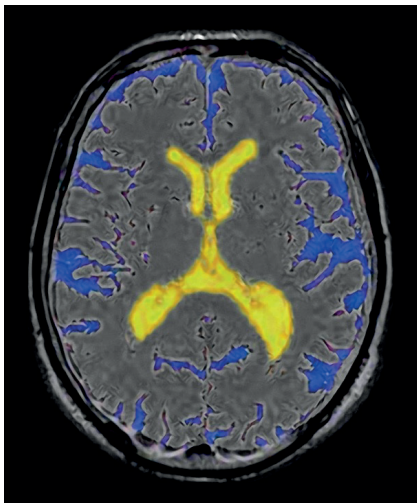


Figure 6.2 Volumetric assessment using SNIPER
Intracranial semi-automated segmentation was based on dual spin-echo (proton attenuation and T2-weighted) and Fluid-Attenuated Inversion Recovery (FLAIR) images. With SNIPER we estimated ventricular volume (VV), sulcal CSF volume (SV), total brain volume (TBV) and total intracranial volume (TICV). TBV/TICV was used as a measure of corrected brain volume.

Covariates

Based on previous studies, we adjusted for a number of potentially confounding demographic and health history factors. Education (primary, secondary, college and university), and smoking status (categorized in this analysis as current or previous smoker versus non-smoker) were assessed with a questionnaire.^{37,38} The presence of depressive symptoms were assessed using the fifteen-item, shortened version of the Geriatric Depression Scale-Shortened (GDSS);³⁹ a score of 6 or greater was classified as high depressive symptomatology.⁴⁰ We adjusted for cardiovascular risk factors and disease as they are reported to be associated with gait and cognition.^{41,42} Systolic and

diastolic blood pressures, measured in supine position, were defined as the first and fifth Korotkoff sounds respectively. History of hypertension was defined as the use of antihypertensive medication, self-reported physician's diagnosis of hypertension, or a systolic blood pressure equal to or higher than 140 mm Hg or a diastolic blood pressure equal to or higher than 90 mm Hg. History of coronary heart disease and peripheral arterial disease (intermittent claudication) were assessed with a questionnaire. Diabetes was defined as a self-reported physician's diagnosis of diabetes, the use of diabetic medications (glucose lowering medications and insulin), which was noted from medication vials brought to the clinic or a fasting blood glucose level ≥ 7.0 mmol/l (equivalent to a fasting blood glucose level of 126 mg/dL, defined as diabetes by the American Diabetes Association). Body mass index was calculated from measured height and weight.

Analytical sample

Of the first 2300 participants, 435 were excluded because no or incomplete MRI images were acquired. The reasons for this were: only participation in a home visit, contraindications for MRI (such as a pacemaker, ocular foreign body or artificial heart valve), claustrophobia or equipment failure. Of the remaining 1865 participants, 697 persons were excluded because of the presence of infarcts (parenchymal defects 4 mm or larger, including Virchow-Robin spaces, and cerebellar infarcts), acute hematomas or mass occupying lesions. The exclusion for the presence of infarcts was based on two reasons. Infarcts may be associated with gait or cognitive impairment as well as bladder dysfunction. Furthermore, infarcts cause an overestimation of sulcal CSF volume. An additional 310 persons were excluded due to failed MR image pre- and post-processing with the SNIPER program, leaving a final sample of 858 persons with complete MRI post-processed data. Compared to those with complete MRI post-processing data, the group of excluded persons was older and contained a higher percentage of men and persons with coronary heart disease, diabetes mellitus and cognitive impairment in either executive function, memory or speed of processing), all significantly different at $p < 0.05$, adjusted for age and sex. There was no significant difference in education, smoking status, BMI, depressive symptomatology, hypertension, bladder dysfunction or gait speed between the included and excluded persons.

Statistical analysis

The higher the value of VV/SV, the more the disproportion between ventricular and sulcal CSF volume. The VV/SV was transformed into standard deviation units (the VV/SV Z-score) and divided into quartiles; the first quartile of the VV/SV Z-score, i.e. the group with the least disproportion, served as the reference group. To discriminate persons with a low performance in the gait test, persons were divided into quartiles of the gait

variables. The upper quartile in either normal or fast gait was defined as gait impairment. The lowest quartile of each of the cognitive composites was classified as impairment in that ability. Impairment in either executive function, memory or speed of processing was classified as cognitive impairment. Bladder dysfunction was classified as urinary urgency or incontinence unrelated to coughing, sneezing, lifting or urge.

We used logistic regressions to examine the association of the VV/SV Z-score to gait impairment, cognitive impairment and bladder dysfunction. We also examined the association of combinations of overall gait impairment, cognitive impairment and bladder dysfunction to quartiles of the VV/SV Z-score. Two models were tested; the first model adjusted for age and sex; the second model had additional adjustments for education, smoking status, body mass index, depressive symptomatology, coronary heart disease, hypertension, diabetes mellitus, peripheral arterial disease, white matter hyperintensity volume and corrected brain volume (SPSS, version 11.5; SPSS Inc., Chicago, IL).

Results

The mean, raw VV/SV for the entire population of 858 was 0.16 (standard deviation: 0.07, range: 0.04 - 0.71). The distribution of VV/SV is presented in Figure 6.3, with image examples from each of the four quartiles in Figure 6.4. Persons in the lowest quartile of VV/SV Z-score are younger and consist of relatively fewer men, but otherwise were not significantly different in the characteristics shown in Table 6.1.

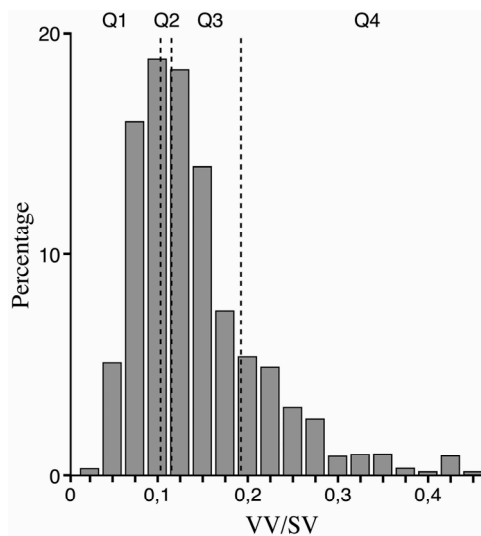


Figure 6.3 Distribution of VV/SV
This histogram shows the distribution of VV/SV in our study population. The vertical lines indicate borders between quartiles.

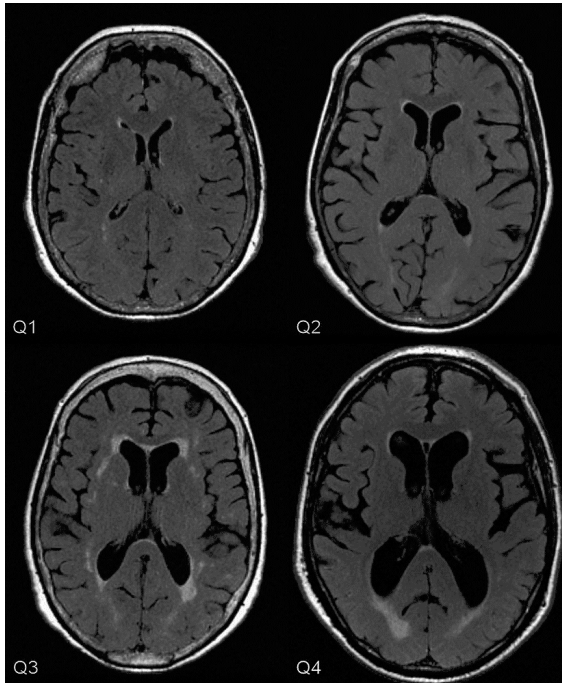


Figure 6.4 Examples of MRI images
Examples of MRI images for persons in the first, second, third and fourth quartile of the VV/SV Z-score.

Table 6.1 Participant characteristics by quartile of the VV/SV Z-score: AGES-Reykjavik Study

	Quartiles of the VV/SV Z-score			
	1 (n = 214)	2 (n = 215)	3 (n = 215)	4 (n = 214)
Age, mean, y (Std)	73.4 (5.0)	74.8 (5.1)	75.4 (5.4)	76.4 (5.5)
Men, %	27	37	37	42
Education, % only primary education	22	22	22	22
Ever smokers, %	60	61	61	58
Body Mass Index, mean (Std)	27.5 (4.4)	26.5 (3.9)	27.4 (4.6)	26.3 (4.5)
Depression symptomatology, %	4	7	6	6
History of coronary heart disease, %	18	24	16	18
Hypertension, %	69	68	64	67
Diabetes mellitus, %	7	7	9	8
Peripheral arterial disease, %	4	4	5	3

Compared to the lowest quartile, those in the top three quartiles were older and more likely to be male. Depression symptomatology is defined as GDSS score of 6 and over. There are no significant trends across quartiles after adjustment for age and sex.

Of the 858 persons, 16.1 percent had both gait impairment and cognitive impairment, 7 percent had both gait impairment and bladder dysfunction, 7 percent had both cognitive impairment and bladder dysfunction, and 4 percent had the complete cluster of symptoms that, as well as in other diseases, typically appear combined in NPH. For all except the bladder dysfunction, the prevalence of impaired individuals increased with increasing quartile of VV/SV (Table 6.2).

Mean scores for each of the individual cognitive tests by quartile of the VV/SV ratio are presented in Table 6.3. Trend tests ($p = 0.05$) show that normal gait speed, fast gait speed, CANTAB Spatial Working Memory, Stroop 3, Immediate Recall, Delayed Recall, DSST, Figure Comparison, Stroop 1 and Stroop 2 show a greater impairment with increasing VV/SV ratio. Table 6.3 also shows the prevalence of dementia for each quartile of the Z-score VV/SV ratio. The prevalence of dementia moderately increases with an increase of the VV/SV ratio.

Compared to the lowest quartile, the highest quartile of the VV/SV Z-score, was associated with overall gait impairment (OR 1.9, 95% CI 1.1 – 3.3; Model 2; Table 6.4). The trend of increasing overall gait impairment with increasing VV/SV Z-score was significant ($p = 0.04$; Model 2; Table 6.4). Compared to the lowest quartile, the highest quartile of the VV/SV Z-score was associated with cognitive impairment (OR 1.8, 95% CI 1.1 – 3.0; Model 2; Table 6.4), but not a specific type of cognitive function. In addition, there was a significant trend of increasing cognitive impairment with increasing VV/SV Z-score ($p = 0.008$; Model 2; Table 6.4). There was an association of bladder dysfunction to the second quartile of VV/SV Z-score; but there was no trend across quartiles (Table 6.4).

Compared to the lowest quartile, the highest quartile of the VV/SV Z-score was associated with a combination of gait impairment and cognitive impairment (OR 2.6, 95% CI 1.3 – 5.3; Model 2; Table 6.5). There was a significant trend for a combination of gait impairment and cognitive impairment with increasing VV/SV Z-score ($p = 0.006$; Model 2; Table 6.5).

In general, having a combination of bladder dysfunction with either gait impairment or cognitive impairment was not associated with increasing quartiles of VV/SV Z-score (Table 6.5). Compared to the lowest quartile, only the third quartile of the VV/SV Z-score was significantly associated with the triad of gait impairment, cognitive impairment and bladder dysfunction (OR 4.9, 95% CI 1.4 – 18.0). There was a modest trend ($p = 0.07$; Model 2; Table 6.5) of more persons with the complete cluster of symptoms with a higher VV/SV index.

Table 6.2 Percent distribution of impaired cases by quartile of VV/SV Z-score: AGES-Reykjavik Study

	Quartiles of the VV/SV Z-score			
	1	2	3	4
Mean VV/SV score	0.09	0.12	0.16	0.26
Mean VV/SV Z-score	1.2	1.7	2.3	3.6
Gait impairment	40 (19%)*	51 (24%)*	55 (26%)*	77 (37%)*
Executive function impairment	27 (13%)	43 (21%)	47 (23%)	51 (26%)
Memory impairment	27 (14%)	32 (16%)	42 (22%)	51 (28%)
Speed of processing impairment	26 (13%)*	31 (15%)*	45 (21%)*	49 (25%)*
Cognitive impairment	58 (30%)*	70 (36%)*	86 (45%)*	101 (52%)*
Bladder dysfunction	40 (19%)	42 (20%)	59 (28%)	40 (19%)
Gait impairment and cognitive impairment	18 (9%)*	29 (14%)*	39 (19%)*	48 (24%)*
Gait impairment and bladder dysfunction	9 (4%)	11 (5%)	28 (13%)	14 (7%)
Cognitive impairment and bladder dysfunction	11 (5%)	9 (4%)	26 (13%)	17 (8%)
Triad	4 (2%)	4 (2%)	20 (10%)	9 (4%)

Percentages in brackets represent the percentage of the included sample (n = 858). *Significant trend across quartiles after adjustment for age and sex ($P < 0.05$).

Table 6.3 Sample characteristics of individual gait and cognitive tests according to quartiles of the VV/SV Z-score

	Quartiles of the VV/SV Z-score								P _{trend}
	1		2		3		4		
	Mean	SD	Mean	SD	Mean	SD	Mean	SD	
Gait speed* (time in s)									
Normal [†]	-0.30	0.67	-0.21	0.64	-0.16	0.78	0.12	1.00	< 0.001
Fast [†]	-0.23	0.83	-0.14	0.85	-0.16	0.92	0.08	1.03	0.002
Executive function*									
Digits backward	0.23	0.99	0.04	0.98	0.09	1.04	0.02	1.08	0.060
Spatial Working Memory [†]	-0.26	0.89	-0.11	1.02	0.10	0.90	0.02	0.96	< 0.001
Stroop 3 [†]	-0.26	0.76	-0.09	0.95	-0.05	1.02	0.01	0.96	0.003
Memory*									
Immediate recall	0.40	0.97	0.14	0.96	0.06	1.00	-0.10	0.95	< 0.001
Delayed recall	0.39	0.98	0.15	0.98	0.11	0.97	-0.14	0.98	< 0.001
Speed of processing*									
DSST	0.41	0.91	0.25	1.00	0.11	0.98	0.01	1.02	< 0.001
Figure comparison	0.37	0.91	0.20	1.04	0.11	1.00	-0.06	1.00	< 0.001
Stroop 1 [†]	-0.23	0.79	-0.12	1.01	-0.12	0.77	-0.05	0.74	0.037
Stroop 2 [†]	-0.27	0.77	-0.14	1.01	-0.08	0.80	-0.02	0.88	0.002
Dementia (%)	0.47		3.26		3.72		3.27		

*Z-scores (mean for total sample = 0.0, standard deviation for total sample = 1.0); †Lower scores represent better performance.

Table 6.4 Quartiles of the VV/SV Z-score and individual impairments: AGES-Reykjavik Study

	Model 1 Quartiles of the VV/SV Z-score					Model 2 Quartiles of the VV/SV Z-score				
	1	2	3	4	P _{trend}	1	2	3	4	P _{trend}
Gait	1.0	1.3 (0.8-2.2)	1.3 (0.8-2.1)	2.2* (1.4-3.6)	0.002*	1.0	1.2 (0.7-2.0)	1.0 (0.6-1.8)	1.9* (1.1-3.3)	0.04*
Executive function	1.0	1.6 (0.9-2.7)	1.6 (0.9-2.8)	1.6 (0.96-2.8)	0.1	1.0	1.2 (0.7-2.2)	1.4 (0.8-2.6)	1.3 (0.8-2.4)	0.4
Memory	1.0	0.9 (0.5-1.6)	1.3 (0.7-2.3)	1.5 (0.9-2.6)	0.07	1.0	0.9 (0.5-1.8)	1.3 (0.7-2.4)	1.4 (0.7-2.7)	0.2
Speed of processing	1.0	1.1 (0.6-1.9)	1.5 (0.9-2.6)	1.6 (0.9-2.7)	0.048*	1.0	1.0 (0.5-1.9)	1.3 (0.7-2.4)	1.6 (0.8-3.0)	0.1
Cognition	1.0	1.0 (0.6-1.6)	1.4 (0.9-2.2)	1.7* (1.1-2.7)	0.006*	1.0	0.9 (0.6-1.5)	1.4 (0.8-2.3)	1.8* (1.1-3.0)	0.008*
Bladder dysfunction	1.0	1.2 (0.7-1.9)	1.8* (1.2-2.9)	1.2 (0.7-1.9)	0.2	1.0	1.3 (0.7-2.1)	1.7 (0.99-2.8)	1.2 (0.7-2.1)	0.3

The first quartile of the VV/SV Z-score, indicated in the table as 1.0, served as the reference group. Model 1 was adjusted for age and sex. Model 2, the fully adjusted model, was adjusted for age, sex, education, smoking, body mass index, depression, hypertension, coronary heart disease, DM, total WMH volume, history of peripheral artery disease and brain volume corrected for intracranial volume.

*Indicates a significant relationship (P < 0.05).

Table 6.5 Quartiles of the VV/SV Z-score and impairment combinations: AGES-Reykjavik Study

	Model 1 Quartiles of the VV/SV Z-score					Model 2 Quartiles of the VV/SV Z-score				
	1	2	3	4	P _{trend}	1	2	3	4	P _{trend}
Gait + cognition	1.0	1.5 (0.8-2.8)	2.0* (1.1-3.7)	2.5* (1.3-4.6)	0.002*	1.0	1.5 (0.7-3.2)	1.9 (0.9-3.9)	2.6* (1.3-5.3)	0.006*
Gait + bladder dysfunction	1.0	1.2 (0.5-3.1)	3.3* (1.5-7.4)	1.5 (0.6-3.7)	0.09	1.0	1.3 (0.5-3.4)	3.0* (1.2-7.4)	1.6 (0.6-4.3)	0.1
Cognition + bladder dysfunction	1.0	0.8 (0.3-1.9)	2.5* (1.2-5.2)	1.5 (0.7-3.3)	0.06	1.0	0.7 (0.3-1.8)	1.9 (0.8-4.3)	1.3 (0.6-3.3)	0.2
Triad (gait + cognition + bladder dysfunction)	1.0	0.9 (0.2-3.8)	4.9* (1.6-14.8)	1.9 (0.6-6.6)	0.05	1.0	0.9 (0.2-4.3)	4.9* (1.4-18.0)	2.2 (0.5-8.8)	0.07

The first quartile of the VV/SV Z-score, indicated in the table as 1.0, served as the reference group. Model 1 was adjusted for age and sex. Model 2, the fully adjusted model, was adjusted for age, sex, education, smoking, body mass index, depression, hypertension, coronary heart disease, DM, total WMH volume, history of peripheral artery disease and brain volume corrected for total intracranial volume.

*Indicates a significant relationship (P < 0.05).

Discussion

This study examined the association of ventricular dilation relative to sulcal CSF volume with gait, cognitive function and bladder dysfunction in infarct-free older persons from a population-based sample. We found that those in the highest quartile of the VV/SV Z-score, reflecting ventricular dilation, were more likely to have impaired gait and cognition. Those in the highest quartile of the VV/SV Z-score were also more likely to have both impaired gait and impaired cognition. There was no direct relationship between ventricular dilation and bladder dysfunction. The combination of gait impairment, cognitive impairment and bladder dysfunction, the three symptoms that typically appear combined in NPH, was present in 4.4 percent of our study sample. Presence of the complete cluster of symptoms was moderately more frequent as the quartile of VV/SV Z-score increased. These effects were present after adjustment for brain volume corrected for total intracranial volume. All associations were independent of WMH volume, and no differences were found in the prevalence of cardiovascular risk factors between the different quartiles of VV/SV Z-scores.

This study is based on a well-characterized population-based cohort of men and women originally identified in the Reykjavik Study and who participated in the follow-up, the AGES – Reykjavik Study; they were not recruited into the study based on any particular characteristic, such as gait or cognitive impairment. Further, we had a standardized neuropsychological test battery of key cognitive functions and an automatic and highly reproducible segmentation of intracranial CSF volumes. However, it is noted this analytical sample excludes those who were older, more frequently male and who had cerebral infarcts on MRI, potentially limiting the generalizability of our study sample. NPH associated bladder dysfunction is described as urinary urgency or complete disinhibition of bladder function. Previous studies have employed many different questionnaires to classify the NPH type of bladder dysfunction, with the number of questions ranging between 2 and 18. However, an international group of experts recommended the use of a self administered three question incontinence questionnaire (3IQ) with questions similar to ours.⁴³ Our assessment of bladder dysfunction captured a defined set of symptoms similar to those recommended; it is possible that questions on additional symptoms may identify a different group than was identified here.

The association between ventricular dilation and gait impairment was known to exist in persons with NPH, and was also found in our study. In the pathogenesis of NPH, the mechanism by which distended ventricles affect gait, cognition and bladder function is unclear.⁴⁴ One theory is that pressure effects of the distended ventricles are exerted on critical cerebral sites.⁴⁴ The fibers of the corticospinal tract that supply motor function

to the legs pass closest to the lateral ventricles in the corona radiata, which may explain why gait disturbance is usually the first and leading symptom to appear in NPH.^{4,9,45} Of the three impairments, the association between ventricular dilation and gait impairment was the strongest in our study population, consistent with the NPH syndrome.

We also found an association between ventricular dilation and cognitive impairment. Cognitive impairment is usually the second symptom to appear in NPH, and does not occur in all patients with NPH.^{9,10} When there is impairment, the cognitive deficit consists principally of memory impairment, decreased speed of complex information processing or poor executive function.^{4,10,46} While we did not find an association between ventricular dilation and impairment in a specific cognitive ability, ventricular dilation was associated with each of the functions we measured.

We did not find an individual association between the VV/SV Z-score and bladder dysfunction. However, participants in the third quartile of the VV/SV Z score were more likely to have both gait impairment and bladder dysfunction. This may be due to an uneven distribution of persons with both gait impairment and bladder dysfunction among the quartiles (Table 6.2). In addition, it may be possible that persons in the highest quartile of the VV/SV Z-score had difficulties reporting bladder dysfunction due to cognitive impairment. Bladder dysfunction has been described as a late stage symptom in NPH,¹⁰ suggesting it would only be associated with VV/SV Z-score when both gait impairment and cognitive impairment are present.

The exact incidence and prevalence of NPH in the general population is not known.⁹ This is partly explained by inconsistent definitions of NPH, which rely on clinical and neuroimaging criteria in some series, and is confirmed by improvement after ventricular shunting in others.¹⁰ We found a 4.4 percent prevalence of a combination of gait impairment, cognitive impairment and bladder dysfunction. This number is limited by the inability to control for other causes of gait impairment, such as lumbar canal stenosis, or other causes of bladder dysfunction.⁸

In conclusion, in our population-based sample of infarct-free men and women, ventricular dilation, the radiological hallmark of NPH, can be observed frequently and, similar to NPH, this phenomenon is associated with cognitive and gait impairment, and sometimes bladder dysfunction. Whether and how often symptomatic individuals with ventricular dilation from the general population could benefit from ventricular shunting remains to be determined. The quantitative measure of ventricular dilation presented in this study would be a useful tool for future studies addressing this question.

Acknowledgments

The authors thank K. Siggeirsdóttir and M. Jónsdóttir for their contributions to the assessment of gait and cognition, T. Aspelund and M. Chang for their support in data management and J.A.L. Vanneste for reviewing the manuscript. This study has been funded by NIH contract N01-AG-12100, the NIA Intramural Research Program, Hjartavernd (the Icelandic Heart Association), and the Althingi (the Icelandic Parliament).

References

1. Drayer BP. Imaging of the aging brain. Part I. Normal findings. *Radiology*. 1988; 166:785-796
2. Kurihara Y, Simonson TM, Nguyen HD et al. MR imaging of ventriculomegaly--a qualitative and quantitative comparison of communicating hydrocephalus, central atrophy, and normal studies. *J Magn Reson Imaging*. 1995; 5:451-456
3. Schmidt R, Launer LJ, Nilsson LG et al. Magnetic resonance imaging of the brain in diabetes: the Cardiovascular Determinants of Dementia (CASCADE) Study. *Diabetes*. 2004; 53:687-692
4. Bradley WG. Normal pressure hydrocephalus: new concepts on etiology and diagnosis. *AJNR Am J Neuroradiol*. 2000; 21:1586-1590
5. Bradley WG, Jr., Scalzo D, Queralt J et al. Normal-pressure hydrocephalus: evaluation with cerebrospinal fluid flow measurements at MR imaging. *Radiology*. 1996; 198:523-529
6. Fishman RA, Dillon WP. Normal pressure hydrocephalus: new findings and old questions. *AJNR Am J Neuroradiol*. 2001; 22:1640-1641
7. Jack CR Jr, Lexa FJ, Trojanowski JQ et al. Normal aging, dementia, and neurodegenerative disease. In: Atlas SW, ed. *Magnetic resonance imaging of the brain and spine*. Vol. 1.3 ed. Philadelphia,PA: Lippincott Williams & Wilkins, 1 A.D.:1177-1240
8. Factora R, Luciano M. Normal pressure hydrocephalus: diagnosis and new approaches to treatment. *Clin Geriatr Med*. 2006; 22:645-657
9. Meier U, Zeilinger FS, Kintzel D. Signs, symptoms and course of normal pressure hydrocephalus in comparison with cerebral atrophy. *Acta Neurochir (Wien)*. 1999; 141:1039-1048
10. Vanneste JA. Diagnosis and management of normal-pressure hydrocephalus. *J Neurol*. 2000; 247:5-14
11. Rubenstein LZ, Josephson KR, Robbins AS. Falls in the nursing home. *Ann Intern Med*. 1994; 121:442-451
12. Sudarsky L. Geriatrics: gait disorders in the elderly. *N Engl J Med*. 1990; 322:1441-1446
13. Hofman A, Ott A, Breteler MM et al. Atherosclerosis, apolipoprotein E, and prevalence of dementia and Alzheimer's disease in the Rotterdam Study. *Lancet*. 1997; 349:151-154
14. Knopman DS, Boeve BF, Petersen RC. Essentials of the proper diagnoses of mild cognitive impairment, dementia, and major subtypes of dementia. *Mayo Clin Proc*. 2003; 78:1290-1308
15. Anger JT, Saigal CS, Stothers L et al. The prevalence of urinary incontinence among community dwelling men: results from the National Health and Nutrition Examination survey. *J Urol*. 2006; 176:2103-2108
16. Brown JS, Nyberg LM, Kusek JW et al. Proceedings of the National Institute of Diabetes and Digestive and Kidney Diseases International Symposium on Epidemiologic Issues in Urinary Incontinence in Women. *Am J Obstet Gynecol*. 2003; 188:S77-S88
17. Babikian V, Ropper AH. Binswanger's disease: a review. *Stroke*. 1987; 18:2-12
18. Bennett DA, Wilson RS, Gilley DW et al. Clinical diagnosis of Binswanger's disease. *J Neurol Neurosurg Psychiatry*. 1990; 53:961-965
19. Pantoni L, Garcia JH. The significance of cerebral white matter abnormalities 100 years after Binswanger's report. A review. *Stroke*. 1995; 26:1293-1301
20. Andresdottir MB, Sigfusson N, Sigvaldason H et al. Erythrocyte sedimentation rate, an independent predictor of coronary heart disease in men and women: The Reykjavik Study. *Am J Epidemiol*. 2003; 158:844-851
21. Danesh J, Wheeler JG, Hirschfield GM et al. C-reactive protein and other circulating markers of inflammation in the prediction of coronary heart disease. *N Engl J Med*. 2004; 350:1387-1397
22. Saczynski JS, Jonsdottir MK, Garcia ME et al. Cognitive impairment: an increasingly important complication of type 2 diabetes: the age, gene/environment susceptibility--Reykjavik study. *Am J Epidemiol*. 2008; 168:1132-1139
23. Cummings SR, Nevitt MC, Browner WS et al. Risk factors for hip fracture in white women. Study of Osteoporotic Fractures Research Group. *N Engl J Med*. 1995; 332:767-773

24. Guralnik JM, Simonsick EM, Ferrucci L et al. A short physical performance battery assessing lower extremity function: association with self-reported disability and prediction of mortality and nursing home admission. *J Gerontol*. 1994; 49:M85-M94
25. Ostir GV, Markides KS, Black SA et al. Lower body functioning as a predictor of subsequent disability among older Mexican Americans. *J Gerontol A Biol Sci Med Sci*. 1998; 53:M491-M495
26. Fitzpatrick AL, Buchanan CK, Nahin RL et al. Associations of gait speed and other measures of physical function with cognition in a healthy cohort of elderly persons. *J Gerontol A Biol Sci Med Sci*. 2007; 62:1244-1251
27. Inzitari M, Newman AB, Yaffe K et al. Gait speed predicts decline in attention and psychomotor speed in older adults: the health aging and body composition study. *Neuroepidemiology*. 2007; 29:156-162
28. Saczynski JS, Jonsdottir MK, Sigurdsson S et al. White matter lesions and cognitive performance: the role of cognitively complex leisure activity. *J Gerontol A Biol Sci Med Sci*. 2008; 63:848-854
29. Wechsler D. The measurement and appraisal of adult intelligence. *Manual for the Wechsler Adult Intelligence Scale*. New York: Psychological Corporation, 1955
30. Robbins TW, James M, Owen AM et al. Cambridge Neuropsychological Test Automated Battery (CANTAB): a factor analytic study of a large sample of normal elderly volunteers. *Dementia*. 1994; 5:266-281
31. Stroop JR. Studies of interference in serial verbal reactions. *J Exp Psychol*. 1935; 18:643-662
32. Delis DC, Kramer JH, Kaplan E et al. The California Verbal Learning Test - Research edition. New York: Psychological Corporation, 1987
33. Salthouse TA, Babcock RL. Decomposing adult age differences in working memory. *Dev Psychol*. 1991; 27:763-776
34. Corkill RG, Cadoux-Hudson TA. Normal pressure hydrocephalus: developments in determining surgical prognosis. *Curr Opin Neurol*. 1999; 12:671-677
35. Admiraal-Behloul F, van den Heuvel DM, Olofsen H et al. Fully automatic segmentation of white matter hyperintensities in MR images of the elderly. *Neuroimage*. 2005; 28:607-617
36. Jenkinson M, Smith S. A global optimisation method for robust affine registration of brain images. *Med Image Anal*. 2001; 5:143-156
37. Aevarsson O, Skoog I. A longitudinal population study of the mini-mental state examination in the very old: relation to dementia and education. *Dement Geriatr Cogn Disord*. 2000; 11:166-175
38. Anstey K, Christensen H. Education, activity, health, blood pressure and apolipoprotein E as predictors of cognitive change in old age: a review. *Gerontology*. 2000; 46:163-177
39. Yesavage JA. Geriatric Depression Scale. *Psychopharmacol Bull*. 1988; 24:709-711
40. Lichtenberg PA, Ross T, Millis SR et al. The relationship between depression and cognition in older adults: a cross-validation study. *J Gerontol B Psychol Sci Soc Sci*. 1995; 50:25-32
41. Klein BE, Klein R, Knudtson MD et al. Frailty, morbidity and survival. *Arch Gerontol Geriatr*. 2005; 41:141-149
42. Nash DT, Fillit H. Cardiovascular disease risk factors and cognitive impairment. *Am J Cardiol*. 2006; 97:1262-1265
43. Fisher CM. Hydrocephalus as a cause of disturbances of gait in the elderly. *Neurology*. 1982; 32:1358-1363
44. Graff-Radford NR, Godersky JC. Normal-pressure hydrocephalus. Onset of gait abnormality before dementia predicts good surgical outcome. *Arch Neurol*. 1986; 43:940-942
45. Gallia GL, Rigamonti D, Williams MA. The diagnosis and treatment of idiopathic normal pressure hydrocephalus. *Nat Clin Pract Neurol*. 2006; 2:375-381

6

Disproportionate ventricular dilatation in the elderly could be a manifestation of small vessel disease

Submitted

W.M. Palm
J. van der Grond
J.R. Milles
S. Sigurdsson
G. Eiriksdottir
V. Gudnason
L.J. Launer
M.A. van Buchem

Abstract

Ventricular dilatation out of proportion to the sulcal cerebrospinal fluid (CSF) volume is a characteristic of normal pressure hydrocephalus (NPH), but has also been described in the general population. We hypothesized that disproportionate ventricular dilatation could be caused by atrophy of the white matter based on small vessel disease. Our aim was to investigate the relationship between white matter hyperintensity (WMH) volume and disproportionate ventricular dilatation.

Data are based on 858 persons (35.4 % men, age range 66-92 years) who participated in the Age, Gene/Environment Susceptibility Study - Reykjavik Study. MRI was followed by segmentation of ventricular, sulcal and WMH volume. Disproportionate ventricular dilatation was measured using the ratio of ventricular volume and sulcal CSF volume, VV/SV. Linear regressions were used to study the relationship between WMH volume, ventricular volume, sulcal CSF volume, and VV/SV, adjusted by age, sex, smoking, hypertension, cardiac disease, blood cholesterol, diabetes, body mass index and total intracranial volume.

WMH volume was positively correlated with ventricular volume and VV/SV (both at $p < 0.001$). However, WMH volume showed a negative correlation with sulcal CSF volume ($p < 0.001$).

Our findings suggest that dilatation of the ventricles in patients with white matter hyperintensities may not be a mere reflection of small vessel disease based atrophy, but that it could be, at least partly, based on active expansion of the ventricles. This unexpected finding offers a new perspective on the pathophysiology of NPH.

Introduction

Disproportionate ventricular dilatation is the radiological hallmark of normal pressure hydrocephalus (NPH), a syndrome characterized by a relative increase in ventricular volume and impairment of gait, cognition and sometimes bladder function.¹⁻³ In a population-based study, it was demonstrated that this radiological phenomenon is often observed in the elderly and that it is associated with subclinical impairment.⁴

The cause of disproportionate ventricular dilatation is not known. However, patients with WMH often present with an enlarged ventricular system, as well as symptoms and signs similar to those seen in NPH.⁵⁻⁷ Furthermore, there is firm evidence that WMH in the elderly are based on cerebral small vessel disease (SVD).⁸ Based on these observations, we hypothesized that disproportionate ventricular dilatation is the consequence of selective central atrophy secondary to SVD. Since WMH are one of the main manifestations of SVD, we predicted that WMH would be associated with disproportionate ventricular dilatation.

Materials and methods

Patients

Subjects are participants in the Age, Gene/Environment Susceptibility (AGES) Reykjavik Study; a population study initiated to examine the contribution of genetic susceptibility and gene/environment interaction to phenotypes common in old age. The AGES is an extension of the Reykjavik Study (1967-1994); a prospective study of cardiovascular disease based on a cohort of men and women born 1907-1935 and living in Reykjavik at the time of baseline measure in 1967. All participants in the AGES Study underwent extensive evaluation, including MRI of the brain, neuropsychological testing, physical performance, a standard clinical evaluation, and an in-person questionnaire. This report is based on those participants examined from September 2002 until March 2004 (n = 2,300). The AGES Study was approved by the Icelandic National Bioethics Committee (VSN 00-063), the Icelandic Data Protection Authority, and by the institutional review board of the US National Institutes of Health.⁹ All participants gave written informed consent.

MR image acquisition and post-processing

The MRI acquisition protocol and post-processing has been described in an earlier study.⁴ The analyses required dual spin-echo (proton attenuation and T2-weighted) and Fluid-Attenuated Inversion Recovery (FLAIR) images, which were acquired at a field

strength of 1.5T (GE Medical Systems, Milwaukee, Wisconsin). The dual spin-echo scans were performed with a field of view of 220 mm, a 256 x 256 matrix size, section thickness of 3.0 mm, 54 slices and no slice gap. The FLAIR scans were performed with a field of view of 220 mm, a 256 x 256 matrix size, section thickness of 3.0 mm, 46 slices and no slice gap. All images were checked for cerebral infarcts by an experienced neuroradiologist. WMH segmentation was performed using a validated automatic image analysis pipeline. The algorithm consisted of a multi-spectral tissue classification, that has been described in detail in a previous publication.¹⁰ Areas with increased signal on proton attenuation, T2-weighted and FLAIR images were identified as WMH.

To segment CSF volumes, we used previously described semi-automated segmentation software (SNIPER, Software for Neuro-Image Processing in Experimental Research) that combines knowledge-based fuzzy clustering and region-growing techniques.¹¹ Brain extraction was followed by an automated segmentation procedure that assigned CSF volumes within the skull. CSF belonging to the lateral and third ventricles was manually labeled as ventricular volume. The fourth ventricle was not included in our analysis. The volumetric assessment was repeated for 43 out of 834 subjects (5%) to analyze the intra-rater reliability in our sample. The assessment yielded an intra-class correlation coefficient greater than 0.99, indicating high intra-rater reliability. The program estimated total intracranial volume and total CSF (tCSF) volume. Sulcal CSF volume (SV) was calculated by extracting ventricular CSF volume (VV) from tCSF volume. Ventricular dilatation was expressed as VV/SV. These volumetric measures have been applied in a previous publication.⁴

Covariates

Based on previous studies, we adjusted for possibly confounding demographic (age and sex) and health history factors. Systolic and diastolic blood pressures, measured in supine position, were defined as the first and fifth Korotkoff sounds respectively. History of hypertension was defined as the use of antihypertensive medication or a systolic blood pressure equal to or higher than 140 mm Hg or a diastolic blood pressure equal to or higher than 90 mm Hg. History of coronary heart disease, diabetes mellitus and peripheral arterial disease were assessed with a combination of questionnaire and clinical data, including medication use. Smoking status (current or previous smoker versus non-smoker) and body mass index calculated from measured weight and height were also included as covariates.

Analytical sample

Of the first 2300 participants, 1988 had MRI scans (312 were only examined at home or had contraindications for MRI). Of these 1988, a total of 433 participants were excluded

due to an incomplete MRI scan, an MRI scan of suboptimal image quality precluding successful image post-processing, or automated image post-processing failures. Finally, to avoid a possible overestimation of sulcal CSF volume in the automated segmentation procedure that assigned CSF volumes within the skull, we excluded 697 subjects with significant cerebral or cerebellar infarcts, defined as parenchymal defects with a long axis diameter ≥ 4 mm outside the basal ganglia, the midbrain or the cortex along the path of the medullary arteries, and with a short axis diameter ≥ 4 mm within these areas. This resulted in a sample of 858 subjects with complete MRI post-processed data. Compared to those with complete MRI post-processing data, the group of excluded subjects was older and contained a higher percentage of males and subjects with depressive symptomology, coronary heart disease and diabetes mellitus (all significantly different at $p < 0.05$, adjusted for age and sex).

Statistical analysis

A linear regression analysis was used to study the relationship between WMH volume and ventricular dilatation, adjusted for age, sex, smoking, hypertension, coronary heart disease, diabetes and body mass index (IBM SPSS Statistics, version 20; IBM Corp., Armonk, N.Y.). In addition, linear regression analyses were used to study the relationship between WMH volume and ventricular or sulcal CSF volume, adjusted for total intracranial volume, as well as adjusted for age, sex, smoking, hypertension, coronary heart disease, diabetes and body mass index.

Results

Our study population of 858 persons ranged in age from 66 to 92 years of age, and had a wide variety of cardiovascular risk factors (Table 7.1). Volumetric assessment yielded a mean total intracranial volume of 1738.5 ml, a mean VV of 43.1 ml, a mean sulcal CSF volume of 279.6 ml, and a median WMH volume of 12.3 ml.

The associations between WMH volume, intracranial CSF compartments and disproportionate ventricular dilation are summarized in Table 7.2. WMH volume showed a significant positive association with VV, as well as with VV/SV, independent of demographic and cardiovascular risk factors and intracranial volume (both associations at $p < 0.001$, standardized coefficient beta 0.14 and 0.22 respectively). These findings indicate that increasing WMH was associated with both increasing ventricular volume and increasing disproportionate ventricular dilatation. WMH volume showed a significant negative association with SV, independent of demographic and cardiovascular risk factors and intracranial volume ($p < 0.001$, standardized coefficient

beta – 0.12). These findings indicate that increasing WMH was associated with decreasing sulcal CSF volume. In our adjusted model, none of the individual cardiovascular risk factors showed an independent association with VV/SV.

Table 7.1 Participant characteristics

	n = 858
Age, mean (SD)	75.0 (5.4)
Women (%)	64.6
Current or previous smoker (%)	60.0
Body mass index (SD)	26.9 (4.4)
Coronary heart disease (%)	18.8
Hypertension (%)	67.0
Diabetes mellitus (%)	7.7
Total intracranial volume, mean (ml)	1738.5
Ventricular volume, mean (ml)	43.1
Sulcal CSF volume, mean (ml)	279.6
WMH volume, median (ml)	12.3

Table 7.2 Association between WMH volume, intracranial CSF compartments and disproportionate ventricular dilation

	Beta (95% CI)
Ventricular volume	0.20 (5.09 – 9.48)
Sulcal CSF volume	-0.12 (-16.1 – -7.1)
Ventricular volume / sulcal CSF volume	0.28 (0.03 – 0.04)

After adjusting for age, sex, smoking, body mass index, blood cholesterol, coronary heart disease, hypertension, diabetes mellitus and intracranial volume, WMH volume shows a positive association with ventricular volume and disproportionate ventricular dilation, but a negative association with sulcal CSF volume.

Discussion

We observed that WMH volume has a positive association with both ventricular volume and disproportionate ventricular dilation, but a negative association with sulcal CSF volume. In the present study none of the cardiovascular risk factors (smoking, hypertension, body mass index, coronary heart disease and diabetes mellitus) showed an independent association with VV/SV, or disproportionate ventricular dilatation.

The association between WMH and ventricular dilatation has been extensively studied. A meta-analysis of 48 studies found a significant relation in the majority of studies, but did not find sufficient evidence to indicate that this relation is independent of shared risk factors, including vascular risk factors and age.¹² Subcortical arteriosclerotic encephalopathy (SAE) - a form of small vessel vascular dementia caused by damage to the white matter¹³ - and NPH share a number of characteristics. Ventricular dilatation and an increased WMH load have been described in SAE,⁵⁻⁷ as well as in NPH.^{14,15} Arterial hypertension is found in the majority of patients with SAE,¹⁶ and SAE has been associated with stroke and diabetes.¹⁷ While we did not find an independent association of cardiovascular risk factors with disproportionate ventricular dilatation in the present study, others observed an association between a clinical diagnosis of NPH and arterial hypertension, cardiac disease, peripheral vascular disease, and ischemia in the deep white matter.¹⁸⁻²⁰ Furthermore, autopsy studies revealed that the vast majority of WMH in older persons are based on small vessel disease (SVD).²¹ We hypothesized that widening of the ventricles in the elderly is caused by selective SVD-induced atrophy of the periventricular white matter. The correlation between WMH load and ventricular dilatation that we observed was in line with our hypothesis.

However, in addition to the association between increasing WMH and increasing ventricular volume, we also observed an association between increased WMH load and decreased sulcal CSF volume. This finding was unexpected, since in the case of mere parenchymal loss, the cortical sulci would be expected to widen as well, or, in case the atrophy would be selectively periventricular, stay the same. The increased volume of the ventricles and decreased volume of the sulcal CSF space that we found to be associated with WMH load suggests that the observed ventricular volume increase results from an outward displacement of the brain by expanding ventricles rather than from mere atrophy. This observation sheds new light on the pathophysiology of NPH.

NPH is associated with increased cerebral capillary pulsations,²² and this association could provide an explanation for the relation we observed between expansion of the ventricles and WMH load. The origin of increased capillary pulsations in NPH may be the consequence of systemic arterial disease. Mitchell *et al.* demonstrated that increased stiffening of the aorta, assessed by pulse wave velocity measurements, gives rise to increased propagation of pulsatile energy into the vascular bed of end organs such as kidneys and brain.²³ In addition, they demonstrated that in the elderly increased aortic stiffness, resulting in a similar stiffness of the aorta with respect to the carotids, is associated with microvascular brain damage (visible as WMH) and reduced cognitive performance.²⁴ In a separate study that employed internal carotid artery velocity measurements, evidence was similarly found for an indirect link between blood

pressure and WMH through a shared coassociation with increasing arterial stiffness.²⁵ Apart from giving rise to SVD, increased capillary pulsations in the brain could also provide an explanation for widening of the ventricles. These pulsations are transferred to the intracranial CSF, presumably at the site of the choroid plexus where they cause a pulsatile increase in intraventricular CSF pressure during each systole.²² Increased intraventricular CSF pressure waves could cause an increased transmante pressure gradient, giving rise to higher pressure waves at the periventricular than at the more superficial brain structures. This gradient may lead to enlargement of the ventricular volume through the so-called waterhammer effect, that continuously pushes the ventricular wall outward, ultimately causing ventricular dilatation.²⁶ As the ventricles expand, forcing the brain out against the inner table of the calvarium, the sulci may decrease in size along with an increase of the ventricular volume. It is also conceivable that WMH and widening of the ventricles are not just epiphenomena of systemic arterial disease, but that they influence each other. MR-pathological studies have found that periventricular venous collagenosis - a gradual thickening of the walls of periventricular veins and venules with collagen occurring in normal aging - is increased in brains with WMH.²⁷ In addition to venous collagenosis, MR-pathological studies have found arteriolar tortuosity and reduced vessel density in periventricular WMH.²⁸ MR elastography has found softening of the brain in NPH patients, that was even more pronounced in the periventricular region²⁹ and that partly decreased after shunt placement.³⁰ Though no direct relationship with microvascular changes in the periventricular white matter was implied, it is a theoretical possibility that brains with impaired periventricular white matter will be less able to absorb the systolic pressure waves in the ventricles, resulting in more rapidly increasing and higher – and potentially more damaging – CSF pressure waves during each systole.

The strength of our study includes the nature of the study population, which consists of a cohort of participants in a broad range of age groups, with both clinical and subclinical disease. The study is limited by the absence of participants with significant infarcts, who were excluded to prevent misinterpretation of ventricular and sulcal CSF volumes in our automated segmentation procedure. The group of excluded subjects was relatively older and contained a higher percentage of males and subjects with coronary heart disease and diabetes mellitus. The lack of an independent association in the current study of any cardiovascular risk factor with VV/SV - seeming to refute our hypothesis that ventricular enlargement reflects small vessel disease - may be explained by this truncation. It is possible that inclusion of participants carrying the highest rate of cardiovascular risk factors would have strongly contributed to our findings. Conversely, the fact that the associations described in the current study were observed in younger persons without significant infarcts strengthens our conclusions. An additional

limitation is the lack of measures of intra- or extracranial arterial stiffness, which could provide more direct evidence of the potential contribution of arterial stiffness to ventricular dilatation.

In conclusion, our findings suggest that dilatation of the cerebral ventricles in patients with WMH may not be a mere reflection of SVD-based atrophy, but that it could be, at least partly, based on active expansion of the ventricles. This unexpected finding offers a new perspective on the pathophysiology of NPH.

References

1. Bradley WG. Normal pressure hydrocephalus: new concepts on etiology and diagnosis. *AJNR American Journal of Neuroradiology* 2000;21:1586-90.
2. Fishman RA, Dillon WP. Normal pressure hydrocephalus: new findings and old questions. *AJNR American Journal of Neuroradiology* 2001;22:1640-1.
3. Jack CRJ, Lexa FJ, Trojanowski JQ, Braffman BH, Atlas SW. Normal aging, dementia, and neurodegenerative disease. In: Atlas SW, ed. *Magnetic resonance imaging of the brain and spine*. 3 ed. Philadelphia, PA: Lippincott Williams & Wilkins; 2002:1177-240.
4. Palm WM, Saczynski JS, van der Grond J, et al. Ventricular dilation: association with gait and cognition. *Annals of Neurology* 2009;66:485-93.
5. Babikian V, Ropper AH. Binswanger's disease: a review. *Stroke* 1987;18:2-12.
6. Bennett DA, Wilson RS, Gilley DW, Fox JH. Clinical diagnosis of Binswanger's disease. *Journal of Neurology, Neurosurgery, and Psychiatry* 1990;53:961-5.
7. Pantoni L, Garcia JH. The significance of cerebral white matter abnormalities 100 years after Binswanger's report. A review. *Stroke* 1995;26:1293-301.
8. Wardlaw JM, Smith EE, Biessels GJ, et al. Neuroimaging standards for research into small vessel disease and its contribution to ageing and neurodegeneration. *The Lancet Neurology* 2013;12:822-38.
9. Saczynski JS, Jonsdottir MK, Garcia ME, et al. Cognitive impairment: an increasingly important complication of type 2 diabetes: the age, gene/environment susceptibility--Reykjavik study. *American Journal of Epidemiology* 2008;168:1132-9.
10. Sigurdsson S, Aspelund T, Forsberg L, et al. Brain tissue volumes in the general population of the elderly: the AGES-Reykjavik study. *NeuroImage* 2012;59:3862-70.
11. Admiraal-Behloul F, van den Heuvel DM, Olofsen H, et al. Fully automatic segmentation of white matter hyperintensities in MR images of the elderly. *NeuroImage* 2005;28:607-17.
12. Appelman AP, Exalto LG, van der Graaf Y, Biessels GJ, Mali WP, Geerlings MI. White matter lesions and brain atrophy: more than shared risk factors? A systematic review. *Cerebrovascular Diseases* 2009;28:227-42.
13. Akiguchi I, Tomimoto H, Suenaga T, Wakita H, Budka H. Alterations in glia and axons in the brains of Binswanger's disease patients. *Stroke* 1997;28:1423-9.
14. Inatomi Y, Yonehara T, Hashimoto Y, Hirano T, Uchino M. Correlation between ventricular enlargement and white matter changes. *Journal of Neurological Sciences* 2008;269:12-7.
15. Krauss JK, Regel JP, Vach W, et al. White matter lesions in patients with idiopathic normal pressure hydrocephalus and in an age-matched control group: a comparative study. *Neurosurgery* 1997;40:491-5.
16. Loeb C. Binswanger's disease is not a single entity. *Neurological Sciences* 2000;21:343-8.
17. Jellinger KA, Attems J. Prevalence and pathology of vascular dementia in the oldest-old. *Journal of Alzheimers Disease* 2010;21:1283-93.
18. Boon AJ, Tans JT, Delwel EJ, et al. Dutch Normal-Pressure Hydrocephalus Study: the role of cerebrovascular disease. *Journal of Neurosurgery* 1999;90:221-6.
19. Bradley WG, Jr., Whittemore AR, Watanabe AS, Davis SJ, Teresi LM, Homyak M. Association of deep white matter infarction with chronic communicating hydrocephalus: implications regarding the possible origin of normal-pressure hydrocephalus. *AJNR American Journal of Neuroradiology* 1991;12:31-9.
20. Krauss JK, Regel JP, Vach W, Droste DW, Borremans JJ, Mergner T. Vascular risk factors and arteriosclerotic disease in idiopathic normal-pressure hydrocephalus of the elderly. *Stroke* 1996;27:24-9.
21. Fernando MS, Simpson JE, Matthews F, et al. White matter lesions in an unselected cohort of the elderly: molecular pathology suggests origin from chronic hypoperfusion injury. *Stroke* 2006;37:1391-8.
22. Greitz D. Radiological assessment of hydrocephalus: new theories and implications for therapy. *Neurosurgery Review* 2004;27:145-65.

23. Mitchell GF. Effects of central arterial aging on the structure and function of the peripheral vasculature: implications for end-organ damage. *Journal of Applied Physiology* (1985) 2008;105:1652-60.
24. Mitchell GF, van Buchem MA, Sigurdsson S, et al. Arterial stiffness, pressure and flow pulsatility and brain structure and function: the Age, Gene/Environment Susceptibility--Reykjavik study. *Brain* 2011;134:3398-407.
25. Aribisala BS, Morris Z, Eadie E, et al. Blood pressure, internal carotid artery flow parameters, and age-related white matter hyperintensities. *Hypertension* 2014;63:1011-8.
26. Bateman GA. Vascular compliance in normal pressure hydrocephalus. *AJNR American Journal of Neuroradiology* 2000;21:1574-85.
27. Brown WR, Moody DM, Challa VR, Thore CR, Anstrom JA. Venous collagenosis and arteriolar tortuosity in leukoaraiosis. *Journal of Neurological Sciences* 2002;203-204:159-63.
28. Black S, Gao F, Bilbao J. Understanding white matter disease: imaging-pathological correlations in vascular cognitive impairment. *Stroke* 2009;40:S48-S52.
29. Streitberger KJ, Wiener E, Hoffmann J, et al. In vivo viscoelastic properties of the brain in normal pressure hydrocephalus. *NMR Biomed* 2011;24:385-92.
30. Freimann FB, Streitberger KJ, Klatt D, et al. Alteration of brain viscoelasticity after shunt treatment in normal pressure hydrocephalus. *Neuroradiology* 2012;54:189-96.

Summary and conclusions

The general objective of this thesis was to study the causes and consequences of ventricular dilatation in aging. For this purpose, we used ventricular shape analysis to study potential new MRI markers of cognitive decline in aging, subjective memory complaints and AD. In addition, we designed a volumetric measure that may objectively quantify the disproportionate ventricular dilatation that is characteristic of NPH. We investigated the value of this measure for the selection of candidates with NPH for ventricular shunting, studied its association with NPH-like symptoms in the general population and used the measure to explore a possible cardiovascular origin of cerebral ventricular dilatation.

In chapter 2 a method of modeling and analyzing localized shape variations of ventricles was applied to a wide spectrum of cognitive levels. Each participant was assessed with the Mini-Mental State Examination (MMSE), yielding a study sample ranging from cognitively healthy to mild cognitive impairment, and from mild to advanced AD. The severity of periventricular atrophy was estimated as local enlargement of the ventricular surface relative to an average normal subject. We found that the severity of atrophy showed good correlation with MMSE score in the left thalamus, the left temporal horn, the left corona radiata, and the right caudate nucleus, increasing the number of potential biomarkers by means of ventricular shape analysis.

In chapter 3 the method of ventricular shape modeling was directed towards investigating possible local shape differences between cognitively healthy and persons with subjective memory complaints. In this explorative study, we found outward displacement of the ventricular surface adjacent to the thalamus and the corona radiata in persons with subjective memory complaints, compared with controls, suggesting that these structures may be involved in the development of subjective memory complaints. In addition, uncorrected results showed tentative evidence of local shape differences in the ventricular surface of the corpus callosum, hippocampus (inferior temporal horn), and amygdala (superior temporal horn).

Shunt surgery remains the standard treatment for NPH, despite high morbidity rates and lack of evidence indicating that shunt placement is effective in the management of this condition. Many diagnostic procedures have been described that may increase the probability of selecting the appropriate candidates for shunt surgery. In chapter 4 we studied the potential of volumetric assessment to distinguish between patients who respond to ventricular shunt surgery and those who do not. The preoperative ratio of ventricular volume and sulcal CSF volume was correlated with postoperative improvement in gait impairment, cognitive impairment, and bladder function. We found no difference in the mean preoperative ratio of ventricular volume and sulcal CSF

volume between subjects who improved on gait, cognition or bladder function and those who did not. This indicates that volumetric assessment has no predictive value in differentiating between NPH patients who will respond to shunt surgery and those who do not.

In chapter 5 we examined the association of disproportionate ventricular dilatation (expressed as the upper quartile of the ratio of ventricular volume and sulcal CSF volume) with gait impairment, cognitive impairment, and bladder dysfunction in a cohort of elderly persons from the general population. We found that those with disproportionate ventricular dilatation were more likely to have impaired gait and cognition. In addition, they were also more likely to have both impaired gait and impaired cognition. These associations were independent of white matter hyperintensity (WMH) volume. The presence of the radiological hallmark of NPH in persons with NPH triad symptoms in the general population raises the question whether more individuals could benefit from ventricular shunting.

Elaborating on earlier studies that suggested a vascular origin of disproportionate ventricular dilatation in NPH, in chapter 6 we hypothesized that ventricular volume out of proportion to sulcal CSF volume is caused by white matter atrophy resulting from small vessel disease. In order to quantify disproportionate ventricular dilatation, we used the ratio of ventricular volume and sulcal CSF volume (VV/SV) that was described in chapters 4 and 5. WMH volume was chosen to represent small vessel disease. We found that WMH volume was positively correlated with both ventricular volume and sulcal CSF volume. However, WMH volume showed a negative correlation with sulcal CSF volume. Our findings suggest that dilatation of the ventricles in patients with white matter hyperintensities is not a mere reflection of small vessel disease based atrophy, but that it may, at least partly, be based on active expansion of the ventricles. This unexpected finding sheds new light on the pathophysiology of NPH.

Future studies

Early detection

As our explorative study on ventricular shape differences in persons with subjective memory complaints discovered, anatomical differences compared to controls could be detected using ventricular shape analysis in the absence of objective changes in cognitive impairment. Further studies are necessary to investigate its possible value for the early detection of neurodegenerative disorders that are characterized by localized

or general cerebral atrophy, such as Frontotemporal Dementia and Parkinson's Disease dementia.

Arterial stiffness

The theory of a vascular origin of NPH, which was supported by the findings of chapter 6, deserves further exploration with the inclusion of other parameters of arteriosclerosis and mechanical stress such as arterial stiffness. Studies of arterial stiffness in persons with disproportionate ventricular dilation could reinforce the hypothesis that propagation of pulsatile energy into the vascular bed of end organs such as the brain can lead to microvascular brain damage. Further knowledge of the relationship between arterial stiffness and disproportionate ventricular dilation could perhaps aid in the selection of candidates for shunt surgery.

Multimodality approach

The studies set out in this thesis are all based on post-processing of qualitative 1.5T based MRI images. Further possibilities for the study of intracranial CSF compartments lie in the field of higher field imaging (3T and up), as well as a combined approach using quantitative MRI techniques like brain perfusion imaging, phase-contrast cine MRI and MR elastography. In addition, data from neuroimaging studies combined with cerebrospinal fluid markers (amino acids, viscosity, pressure) or serum markers may lead to the discovery of new biomarkers of treatable NPH or the refinement of existing ones.

Longitudinal studies

The available literature on neuroimaging in Normal Pressure Hydrocephalus has until now focused on cross-sectional studies of ventricular dilatation, with the cause of dilatation being inferred from a number of features including the proportion between ventricular volume and sulcal CSF volume, as well as aqueductal stroke volume, the integrity of the periventricular white matter and the absence of a CSF flow obstruction. Longitudinal studies may be helpful in determining whether changes in the shape and size of the ventricular system occur due to (intermittently) elevated cerebrospinal fluid pressure or brain parenchyma loss leading to compensatory enlargement of CSF spaces.

Samenvatting en conclusies

De algemene doelstelling van dit proefschrift was het onderzoeken van de oorzaken en gevolgen van ventriculaire dilatatie bij veroudering. Hiervoor hebben we de vorm van de ventrikels geanalyseerd om potentiële nieuwe MRI markers voor cognitieve achteruitgang te bestuderen bij veroudering, subjectieve geheugenklachten en de Ziekte van Alzheimer. Daarnaast hebben we een volumetrische maat ontworpen die op objectieve wijze de disproportionele ventriculaire dilatatie kan kwantificeren die karakteristiek is voor NPH (Normal Pressure Hydrocephalus). We hebben de waarde van deze maat onderzocht voor het selecteren van kandidaten met NPH ten behoeve van het plaatsen van een ventriculaire shunt, evenals de associatie van deze maat met in de algemene populatie voorkomende bij NPH passende symptomen en hebben de maat gebruikt om een mogelijke cardiovasculaire origine van cerebrale ventriculaire dilatatie te onderzoeken.

In hoofdstuk 2 werd een methode voor modellering en analyse van lokale variaties in ventriculaire vorm toegepast bij een breed spectrum van cognitieve niveaus. Bij elke deelnemer werd de Mini-Mental State Examination (MMSE) afgenomen, waardoor de onderzoekspopulatie ingedeeld kon worden van cognitief gezond tot milde cognitieve achteruitgang en van milde tot geavanceerde Ziekte van Alzheimer. De mate van periventriculaire atrofie werd gedefinieerd als lokale vergroting van het ventriculaire oppervlak ten opzichte van de gemiddelde normale deelnemer. We stelden vast dat de mate van atrofie goed correleerde met MMSE score ter plaatse van de linker thalamus, de linker temporaal hoorn, de linker corona radiata en de rechter nucleus caudatus. Deze anatomische gebieden kunnen in de toekomst wellicht toegevoegd worden aan de lijst van erkende ventriculaire biomarkers.

In hoofdstuk 3 werd de methode van analyse van de ventriculaire vorm toegepast voor het onderzoeken van mogelijke lokale verschillen in ventriculaire vorm tussen cognitief gezonden en personen met subjectieve geheugenklachten. In deze exploratieve studie constateerden we buitenwaartse verplaatsing van het ventriculaire oppervlak grenzend aan de thalamus en de corona radiata bij personen met subjectieve geheugenklachten in vergelijking tot controles, hetgeen suggereert dat deze structuren mogelijk betrokken zijn bij de ontwikkeling van subjectieve geheugenklachten. Daarnaast toonden ongecorrigeerde resultaten tentatief bewijs voor lokale vorm verschillen in het ventriculaire oppervlak van het corpus callosum, de hippocampus (inferieure temporaalhoorn) en amygdala (superieure temporaalhoorn).

Shunt chirurgie maakt nog steeds onderdeel uit van de reguliere behandeling van NPH, ondanks een hoge morbiditeit en matig bewijs dat het plaatsen van een shunt effectief is bij de behandeling van deze aandoening. Er zijn meerdere vormen van diagnostiek

beschreven die de kans op het selecteren van geschikte kandidaten voor shunt chirurgie kunnen verhogen. In hoofdstuk 4 onderzochten we het mogelijke voordeel van volumetrische evaluatie voor het differentiëren tussen patiënten die een gunstig effect zouden ondervinden van een ventriculaire shunt en degenen bij wie dit geen nuttige behandeling zou blijken. De pre-operatieve ratio van ventriculair volume en sulcaal CSF (hersenvocht) volume werd gecorreleerd aan postoperatieve verbetering in lopen, cognitie en blaasfunctie. We stelden geen verschil vast in de gemiddelde ratio tussen de personen die post-operatief een verbetering in lopen, cognitie of blaasfunctie ondervonden en de personen bij wie de beperkingen niet verbeterden. Dit geeft aan dat volumetrische evaluatie geen voorspellende waarde heeft bij het differentiëren tussen NPH patiënten die gunstig zullen reageren op shunt chirurgie en degenen die dat niet zullen doen.

In hoofdstuk 5 onderzochten we de associatie tussen disproportionele ventriculaire dilatatie (uitgedrukt als het bovenste kwartiel van de ratio tussen ventriculair volume en sulcaal CSF volume) met loopstoornissen, cognitieve achteruitgang en blaasdysfunctie in een cohort van oudere personen uit de algemene populatie. We stelden vast dat degenen met disproportionele ventriculaire dilatatie meer kans hadden op loopstoornissen of cognitieve achteruitgang. Daarnaast hadden ze meer kans op een combinatie van zowel loopstoornissen als cognitieve achteruitgang. Deze associaties waren onafhankelijk van het volume van witte stof hyperintensiteiten (WMH). De aanwezigheid van het meest karakteristieke radiologische kenmerk van NPH bij personen uit de gehele populatie met symptomen van de NPH trias roept de vraag op of meer personen baat zouden kunnen hebben bij shunt chirurgie.

Voortbordurend op eerdere studies waaruit een mogelijke vasculaire origine van disproportionele ventriculaire dilatatie in NPH bleek, hebben we in hoofdstuk 6 de hypothese geformuleerd dat ventriculair volume in disproporctie met sulcaal CSF volume veroorzaakt wordt door atrofie van de witte stof als gevolg van microangiopathie. Om disproportionele ventriculaire dilatatie te kunnen kwantificeren hebben we de ratio gebruikt van ventriculair volume en sulcaal CSF volume (VV/SV) die eerder beschreven werd in hoofdstukken 4 en 5. WMH volume werd gekozen om microangiopathie te vertegenwoordigen. We stelden vast dat WMH volume positief gecorreleerd was met zowel ventriculair volume als sulcaal CSF. Echter, WMH volume toonde een negatieve correlatie met sulcaal CSF volume. Onze bevindingen suggereren dat dilatatie van de ventrikels bij patiënten met WMH niet uitsluitend een weerspiegeling is van aan microangiopathie gerelateerde atrofie, maar dat die, in ieder geval gedeeltelijk, kan berusten op actieve expansie van de ventrikels. Deze onverwachte bevinding werpt nieuw licht op de pathofysiologie van NPH.

Toekomstige studies

Vroege detectie

Zoals onze exploratieve studie naar veranderingen van de ventriculaire vorm bij personen met subjectieve geheugenklachten liet zien, konden middels analyse van de ventriculaire vorm anatomische verschillen worden waargenomen tussen personen met subjectieve geheugenklachten en controles, terwijl middels cognitieve testen geen objectiveerbare verschillen waarneembaar waren. Verdere studies lijken noodzakelijk om de mogelijke waarde van ventriculaire vorm analyse te onderzoeken bij neurodegeneratieve aandoeningen die gekarakteriseerd worden door lokale of gegeneraliseerde cerebrale atrofie, zoals Frontotemporale Dementie en de Ziekte van Parkinson.

Arteriële stijfheid

De theorie van een vasculaire origine van NPH, welke ondersteund wordt door de bevindingen in hoofdstuk 6, verdient een verdere exploratie met de inclusie van andere parameters van atherosclerose en mechanische stress zoals arteriële stijfheid. Studies naar arteriële stijfheid bij personen met disproportionele ventriculaire dilatatie kunnen wellicht de hypothese versterken dat voortgeleiding van pulsatiele energie naar het vasculaire bed van eindorganen zoals de hersenen kan leiden tot microvasculaire hersenschade. Een grotere kennis over de relatie tussen arteriële stijfheid en disproportionele ventriculaire dilatatie zou kunnen leiden tot een betere selectie van kandidaten voor shunt chirurgie.

Multimodale benadering

De in dit proefschrift beschreven studies zijn alle gebaseerd op post-processing van kwalitatieve op 1.5T gemaakte MRI onderzoeken. Verdere mogelijkheden voor de studie van intracraniële CSF compartimenten liggen in het veld van beeldvorming met een hogere veldsterkte (3T en hoger), evenals een gecombineerde benadering met kwantitatieve MRI technieken zoals hersenperfusie, fase-contrast dynamische MRI en MR-elastografie. Daarnaast kan data van beeldvorming studies gecombineerd worden met CSF parameters (aminozuren, viscositeit, druk) of serum markers, hetgeen zou kunnen leiden tot de ontdekking van nieuwe biomarkers van behandelbare NPH of verfijning van de huidige.

Longitudinale studies

De beschikbare literatuur met betrekking tot neuroradiologische beeldvorming van NPH heeft zich tot nu toe gericht op cross-sectionele studies van ventriculaire dilatatie, waarbij de oorzaak van de dilatatie wordt afgeleid uit een aantal kenmerken, zoals de

verhouding tussen ventriculair volume en sulcaal CSF volume, het aqueductaal slag volume, de integriteit van de periventriculaire witte stof of het gebrek aan obstructie van afvoer van het CSF. Longitudinale studies kunnen nuttig zijn bij het vaststellen of veranderingen in de vorm en grootte van het ventrikelstelsel optreden als gevolg van (intermitterend) verhoogde CSF druk, dan wel als gevolg van verlies van hersenparenchym waarbij compensatoire vergroting van het ventrikelstelsel ontstaat.

Curriculum vitae

Miguel Palm was born in Valladolid, Spain, on August 26th 1978. After graduating from the Rijnlands Lyceum in Wassenaar in 1996, he was accepted at the University of Leiden to study medicine. For his graduate thesis he conducted research on proton magnetic resonance spectroscopic markers of macrophages in brain tissue in vitro, under the supervision of N.R. Sibson, PhD, and Prof. P. Styles, DPhil, at the Department of Biochemistry of the University of Oxford (The Queen's College, 2000). After graduating in medicine in 2003 he enrolled in a combined PhD and radiology residency program at Leiden University Medical Center under the supervision of Prof. M.A. van Buchem, MD, PhD, and Prof. J.L. Bloem, MD, PhD, leading to a specialist registration as a radiologist in 2011. His training continued at Leiden University Medical Center with a fellowship in neuro- and head and neck radiology, which he completed in 2012. During his residency and fellowship he successfully participated in the 2010-2012 cycle of the Pierre Lasjaunias European Course in Diagnostic and Interventional Neuroradiology, which was concluded with an oral examination at Edinburgh in 2012 for the European Certificate of Neuroradiology. Since 2012 he forms part of the staff of radiologists of Maastricht University Medical Center, where he specializes in neuroradiology, head and neck radiology and abdominal radiology.

Publication list

Palm WM, Ferrarini L, Van der Flier WM, Westendorp RG, Bollen EL, Middelkoop HA, Milles JR, Van der Grond J, Van Buchem MA. Cerebral atrophy in elderly with subjective memory complaints. *J Magn Reson Imaging*. 2013 Aug;38(2):358-64.

Palm WM, Saczynski JS, Van der Grond J, Sigurdsson S, Kjartansson O, Jonsson PV, Eiriksdottir G, Gudnason V, Admiraal-Behloul F, Launer LJ, van Buchem MA; Age, Gene/Environment Susceptibility-Reykjavik Study. Ventricular dilation: association with gait and cognition. *Ann Neurol*. 2009 Oct;66(4):485-93.

Palm WM, Walchenbach R, Bruinsma B, Admiraal-Behloul F, Middelkoop HA, Launer LJ, Van der Grond J, Van Buchem MA. Intracranial compartment volumes in normal pressure hydrocephalus: volumetric assessment versus outcome. *AJNR Am J Neuroradiol*. 2006 Jan;27(1):76-9.

Ferrarini L, **Palm WM**, Olofsen H, Van der Landen R, Van Buchem MA, Reiber JH, Admiraal-Behloul F. Ventricular shape biomarkers for Alzheimer's disease in clinical MR images. *Magn Reson Med*. 2008 Feb;59(2):260-7.

Ferrarini L, **Palm WM**, Olofsen H, Van der Landen R, Blauw GJ, Westendorp RG, Bollen EL, Middelkoop HA, Reiber JH, Van Buchem MA, Admiraal-Behloul F. MMSE scores correlate with local ventricular enlargement in the spectrum from cognitively normal to Alzheimer disease. *Neuroimage*. 2008 Feb 15;39(4):1832-8.

Ferrarini L, **Palm WM**, Olofsen H, Van Buchem MA, Reiber JH, Admiraal-Behloul F. Shape differences of the brain ventricles in Alzheimer's disease. *Neuroimage*. 2006 Sep;32(3):1060-9.

Ferrarini L, Olofsen H, **Palm WM**, Van Buchem MA, Reiber JH, Admiraal-Behloul F. GAMES: growing and adaptive meshes for fully automatic shape modeling and analysis. *Med Image Anal*. 2007 Jun;11(3):302-14.

Van den Heuvel DM, Ten Dam VH, De Craen AJ, Admiraal-Behloul F, Van Es AC, **Palm WM**, Spilt A, Bollen EL, Blauw GJ, Launer L, Westendorp RG, Van Buchem MA; PROSPER Study Group. Measuring longitudinal white matter changes: comparison of a visual rating scale with a volumetric measurement. *AJNR Am J Neuroradiol*. 2006 Apr;27(4):875-8.

Stuckey DJ, Anthony DC, Lowe JP, Miller J, **Palm WM**, Styles P, Perry VH, Blamire AM, Sibson NR. Detection of the inhibitory neurotransmitter GABA in macrophages by magnetic resonance spectroscopy. *J Leukoc Biol*. 2005 Aug;78(2):393-400.